Department of Electrical and Computer Engineering

Adaptive Impedance Matching Circuit for Narrowband Power Line Communication

Chin Pin Rui

This thesis is presented for the Degree of
Master of Philosophy (Electrical and Computer Engineering)
of
Curtin University

October 2013

To the best of my knowledge and belief this thesis contains no material previously published by any other person except where due acknowledgment has been made. This thesis contains no material which has been accepted for the award of any other degree or diploma in any university.

_____ _____

Author Date

Adaptive Impedance Matching Circuit for Narrowband Power Line Communication

by
Chin Pin Rui

Submitted to the Department of Electrical and Computer Engineering
in October, 2013 in partial fulfilment of the
requirements for the degree of
Master of Philosophy (Electrical and Computer Engineering)

ABSTRACT

Power line communication is used in various electrical systems, from high-voltage network to the low-voltage network to transfer information. It is a wired communication that is comparable with the wireless communications because information is modulated with carrier wave before being injected into the communication channels. However, the noise level and impedance mismatch are the main concerns in this technology, particularly in the low voltage network or in residential area. Even though the noise level and the impedance mismatch of a power line communication system can be controlled using a band-pass filter and an impedance matching circuit respectively, the impedances of power line in residential area are time and location dependent, and therefore it is rather difficult to design a circuit that allows maximum power transfer in the system all the time. In this thesis, two new adaptive impedance matching circuits are proposed for narrowband power line communication. These new methodologies are derived based on a RLC and a LCRC circuits. Both concepts are designed to achieve a simpler configuration and a higher matching resolution. It is concluded that the RLC band-pass filter impedance matching network is suitable for the implementation of a narrowband power line communication network that consists of pure resistive impedance. Meanwhile the LCRC impedance matching network is designed to match the signal source impedance to both the resistive and reactive load impedances, thus it is more practical to be used in a residential house.

ACKNOWLEDGEMENTS

Firstly, I would like to express my gratitude to my supervisors, Prof. Nader Nassif Barsoum and Dr. Wong Kiing Ing for their valuable advice and guidance throughout my research. Their continuous feedbacks and encouragements have been a great contribution to the success of this thesis. Although Prof. Nader left Curtin Sarawak during the period of my master degree study, but he never give up on me. He continues his supervision of me through email communication.

From the School of Engineering and Science, I would like to acknowledge my friend, who is also the Laboratory Technical Officer Mr. Daniel Wong Sing Tze and my student, Mr. Wong Tze Jia for assisting me in the experimental analysis of my research. At the same time I would like to acknowledge my colleague, who is also my buddy, Mr. Arthur Wong for assisting me in the theoretical and mathematical analysis of my thesis. In addition to that, I would like to thank my friends, Mr. Peter Wong Jian Sheng and Mr. Alexander Lau for proofreading my thesis. And of course I would like to thank all the lecturers and staffs in the school for their feedbacks, supports and assistance that had contributed greatly to the completion of my thesis.

I also want to grab this opportunity to express my thanks to the great people around me, especially Uncle Chan Kwok Mow, Aunty Sin Sai Liong, Pastor Lim Thien Leong, the Curtin Ministry, Young Adult Ministry and the people from Piasau Baptist Church for their continuous encouragement and support throughout the years.

I wish to thank my family for their love and support towards me. They are my greatest strength and motivation during my thesis-writing. Last but not least, I want to thank God for His unconditional love and blessing to me and the people around me!

Copyright Acknowledgement

Imagery downloaded from the internet has been used in this chapter for testing purposes in accordance with Section 40 of the Australian Copyright Act of 1968, which allows fair dealing of artistic work for purpose of research or study. The following persons are herewith acknowledged as the respective copyright holders:

Test image in Figure 2.1 is © Khairanirani. Test image in Figure 2.2 is © Software Design and Embedded System Tools. Test image in Figure 2.3 is © Don Shaver. Test image in Figure 2.4 is © Hendrik C Ferreira et al. Test image in Figure 2.5 is © Bogdan Baraboi. Test image in Figure 2.6 is © Farrokh Najmabadi. Test image in Figure 2.9 is © IulianRosu.

Test image in Figure 4.2 is © Yuhao Sun. Test image in Figure 4.3 is © Hank Zumbahlen.

Content

List of Figures

List of Tables

CHAPTER 1

INTRODUCTION

In this world of emerging technologies, wireless communications such as infra-red, Bluetooth, and Wi-Fi communications have been implemented in various engineering applications. The main reason of the usage of wireless communication is that users no longer require wired services to reach the hardware. However hardware such as industrial machineries, electrical appliances, automatic gate and security system require electricity through cable connections to the power supplies. Hence, power line communication can be considered as another option of communication by using these cables to perform monitoring and control between the hardware.

Power line communication is the wired communication technology that uses the existing electric wires or cables as a communication channel for a modulated signal to send from a transmitter into a receiver[1]. Similar to wireless communication, power line communication does not require any additional wires or cables to "communicate" between the hardware. However, the signal in wireless communication is deteriorated with transmit through multiple walls and floors. On the other hand, the signal in power line communication does not have the problem because it uses the power supply lines as the communication channel. Therefore, it can be harder to set up a wireless communication network with routers are required to achieve high signal strength. Thus, power line communication has the advantage over wireless communication.

Power line communication can be used in all levels of voltage network. Narrowband power line communication (NB-PLC) technology uses the residential electrical power wiring as a transmission medium to control the lighting and appliances without

installation of additional new wiring. Typical home control devices operate by modulating in a carrier wave of less than 500 kHz in the household wiring at the transmitter [2]. The carrier is modulated by digital signals that is generated from the power line communication transmitter, and sending it to the receiver. Each receiver in the system has an address and can be individually commanded by the signals transmitted over the household wiring and demodulated at the receiver. These devices may be either plugged into regular power outlets, or permanently wired in place [3].

However, power line itself has additive non-white noise and is operating in extremely harsh environment for communication [4, 5]. In low voltage network, the sources of the noise come from the electrical appliances such as light bulb, washing machines, TV and air conditioner. The noise is spread from the electrical appliances into the power line, and therefore it limits the distance of the signal transmit along the power line. At the same time, signal is attenuated by the data reflection along the power line due to the impedance mismatch in the power line network [6, 7]. This impedance mismatch occurs when the value of the channel impedance, which is the electrical appliances in this research, is not equal to the complex conjugate of the source impedance.

In this thesis, two types of adaptive impedance matching circuit methodology had been proposed. The derivations of the circuits are based on a RLC and a LCRC impedance matching networks. These circuits are designed not only to filter the noises in the power line, but at the same time it performs real-time impedance matching with the channel impedance in order to achieve the maximum power transfer in the power line communication system. These methodologies work by digitally varying the values of resistor, inductor and capacitor components to match the impedance in the power line at all times. The values of these components are determined by two new algorithms proposed in this thesis. These methodologies had been tested theoretically using MATLAB and PSIM simulation, and also verified practically through experiment using the laboratory equipment and machineries.

1.1 AIM AND APPROACH

This thesis is concerned with the research into the development of new methodologies for adaptive impedance-matching circuit in narrowband power line communication technology. The derivations of the circuits are based on the two types of impedance matching network, which are RLC and LCRC impedance-matching networks. These circuits are designed to filter the noises in the power line and to perform real time impedance matching in the narrowband power line communication. The objectives of this thesis are:

1. The implementation of two types of methodologies for adaptive impedance matching that is able to filter out the noises and increase the matching resolution in narrowband power line communication.
2. To implement the algorithms for the impedance value measurement in power line communication.
3. To verify the feasibility of the matching circuits through theoretical analysis and practical analysis.

The first aim is addressed by deriving the mathematical equations from both the RLC and LCRC circuit model to calculate the values of the resistor (R), inductor (L) and capacitor (C). These values will then be used by the systems to match the impedance in the power line in order to achieve maximum power transfer for narrowband power line communication. But in order to achieve the above aims, it is crucial to measure the source impedance and the channel impedance of the power line network. In practice, impedance value is a complex number that consists of the resistance, which is the real part, and the reactance, which is the imaginary part. Subsequently, the method used to measure the impedance has to involve some calculations in order to find out both resistance and reactance values. Thus the second aim is addressed by using the suitable algorithm to measure the source and channel impedance in power line communication.

However, since the first and second aims are purely theoretical analysis, it is important to test its feasibility using MATLAB and PSIM simulation, and then perform the practical experiment using the laboratory equipment and machineries to achieve the third aim. The third aim is to verify the feasibility of the matching circuits through theoretical analysis and practical analysis.

1.2 SIGNIFICANCE AND CONTRIBUTION

This thesis makes several main contributions in the field of impedance-matching in narrowband power line communication:

1. The derivation of two new methodologies for adaptive impedance matching circuits that has simpler configuration and higher matching resolution.
2. The simplification of the existing formula given in [8] to measure the impedance value in the power line communication.

The contributions and their significances are detailed in the following.

1.2.1 NEW ALGORITHM OF ADAPTIVE IMPEDANCE MATCHING METHOD

There are a few problems that can be addressed from the current adaptive impedance matching circuit technology. In [8], the turns of the transformer and the value of inductor are altered by sliding the taps, which means it has low resolution of matching unless the number of taps increases. Furthermore, it has high intrinsic parasitic resistance, large size and high cost. Meanwhile for the method used in [9] requires large numbers of capacitors to achieve high resolution of matching. The better solution was shown in [10], where VCGIC is used. This approach has much higher resolution of matching, but with the limitation that it is not performed well in high current load. Therefore, DIRC was introduced, which can operate in both low and high current load

[2]. But this approach requires a high voltage blocking capacitor which has large absolute value of reactance than the inductive reactance in the channel. DIRC bank is needed instead of just a single DIRC to reduce the parasitic resistance of the circuit, which means the circuit becomes more complex.

Therefore in this thesis, new approaches have been introduced to maximise the matching resolution. The RLC and LCRC circuits that consist of different configuration of inductor, capacitor and resistor are used to match the source impedance and channel impedance. The impedance in the power line will be measured to provide feedback value to the digital capacitor, digital resistor and active inductor in order to match the source impedance and channel impedance. As a result, the circuit configurations are simpler, and the noise levels are lower and the matching resolutions are higher.

1.2.2 SIMPLIFICATION OF THE EXISTING FORMULA

The two new methodologies of adaptive impedance matching circuits require the real time values of the source impedance and channel impedance in order to calculate the values of the digital resistor, active inductor and digital capacitor of the RLC and LCRC. This result is crucial to match the impedance. But then it is not easy to find the impedance sensor that can be used to measure impedance value directly. That's why the proposed method in [8] is used and it has been simplified to a simpler form for easier understand on behalf of the users.

1.3 THESIS OUTLINE

This thesis consists of five chapters. In Chapter 2, background information relevant to this thesis is discussed. The overview and the problem statements of power line communication and narrowband power line communication are explained. This chapter continues with a discussion about the solutions to the problem statements. And it concludes with the impedance measurement method and its improvement.

Chapter 3 proposes the RLC band-pass filter adaptive impedance matching circuit methodology. The RLC circuit model and the concept of digital capacitor are explained and the relevant mathematical equations are derived. It also includes the verification of the feasibility of the proposal using MATLAB and PSIM simulation, and experimental verification in laboratory.

The proposed LCRC adaptive impedance matching circuit is explained in Chapter 4. The LCRC circuit model and the concept of active inductor are described in this chapter. It continues with the derivation of the relevant mathematical equations, and the verification of the proposal using MATLAB, PSIM and experimental verification in laboratory.

Chapter 5 concludes the research and outlines open research questions for future work.

CHAPTER 2

BACKGROUND

The scope of this thesis involves power line communication, specifically in the adaptive impedance matching method for narrowband power line communication (NB-PLC). An overview of the current standardisation, technology, application and problem statement of power line communication, particularly in narrowband power line communication is included in this chapter. The solution to the problem statement is also explained in this chapter, which is the literature review of the band-pass filter and impedance matching. The review of the relevant research conducted is given in this chapter too. And of course, the impedance measurement method used in this thesis is included in this chapter as well.

2.1 POWER LINE COMMUNICATION

Power Line Communication is a system that transmits information through a conductor which is generally used for electric power transmission [1,11]. It operates by injecting a modulated carrier signal on the wiring system. Power line communication can be applied at different stages of power distribution system, such as high (>100kV), medium (1 – 100 kV), and low (<1 kV) voltage networks, where in lower voltage distribution network has high difficulty in sending and receiving information through power line. Figure 2.1 illustrates the power line communication network from a power plant to the residential area. Meanwhile Figure 2.2 shows the difference between wireless and power line communication network inside a residential home.

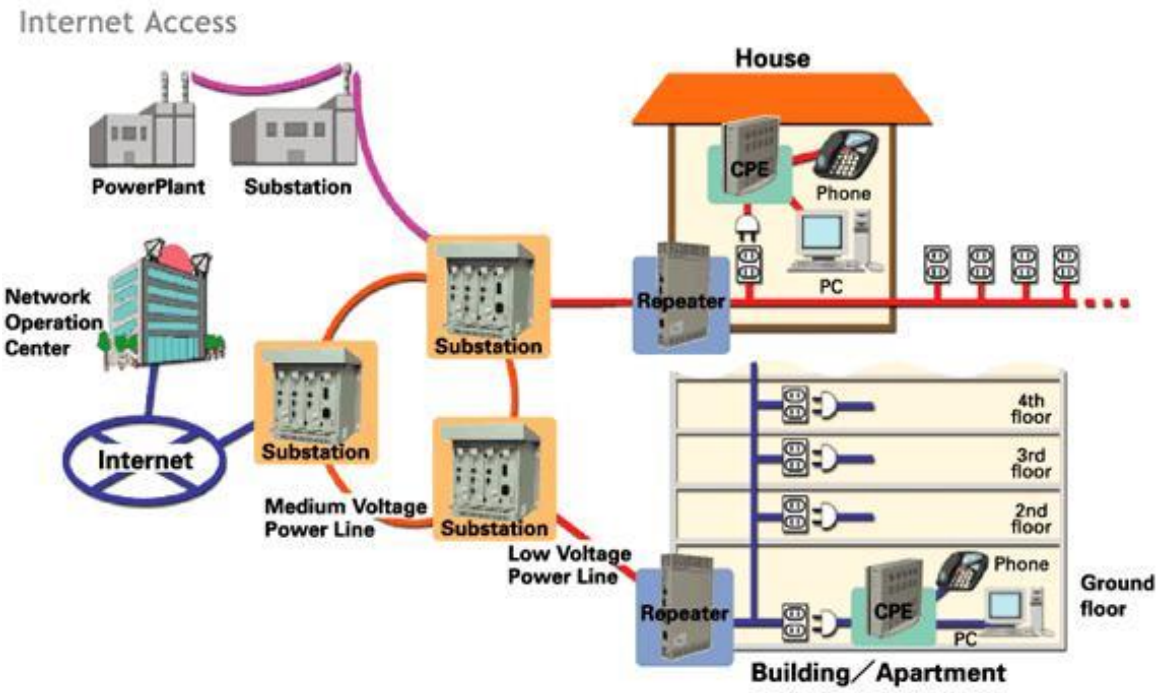

Figure 2.1: Power line communication network at power distribution system[12]

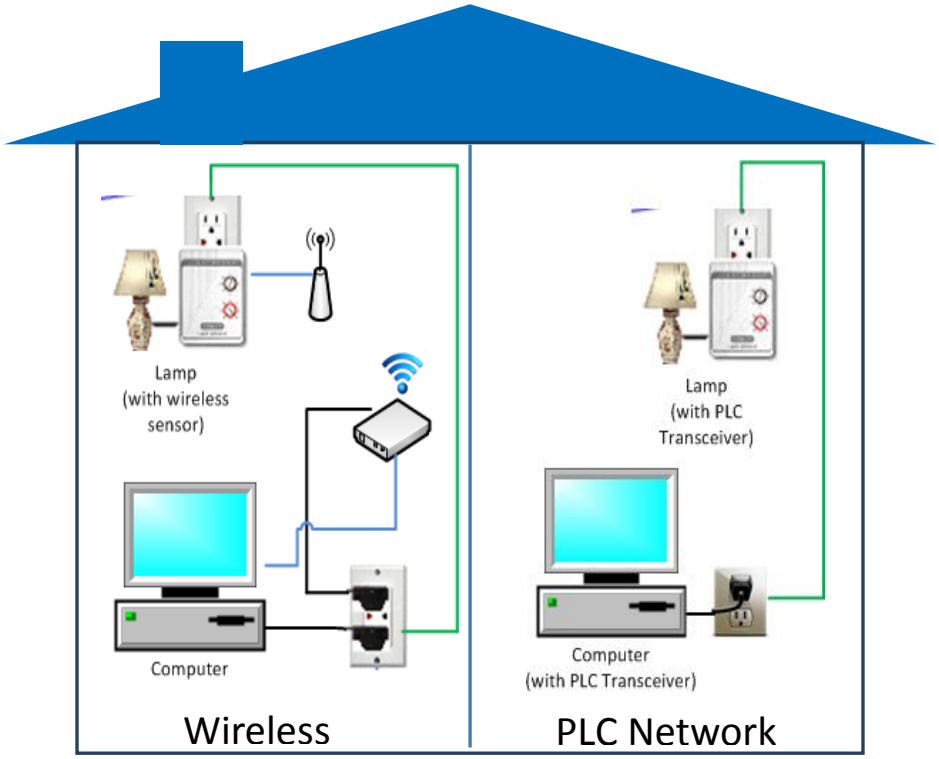

Figure 2.2: Difference between wireless and power line communication network in a house

Power line communication is the only wired communication that is comparable with wireless communication, because both do not require any additional cable for communication. However, power line communication is simpler network as compare with wireless communication, for communication between the electrical appliances in a low voltage (LV) network in a house or office environments. This is because all the electrical appliances are connected to the power line and the signal are transmitted and received between the electrical appliances using the exiting LV network.

There are various applications in a residential home using power line communication, for instance, home automation system, home networking infrastructure, home and utility services, net-washing and e-cooking. By having these applications in a home, the user will be able to access internet using the power cable, monitor the fault, security and power consumption in the house, and perform energy-saving by reducing the energy consumption during peak hours. Apart of that, power line communication can also be implemented in long haul application, such as smart grid, irrigation monitoring and management system in Golf course system, and electro-pneumatic braking system in Association of American Railroads, etc.[13]

There are two classes of power line communication system, namely narrowband power line communication (NB-PLC) and broadband power line communication (BPL). In general, NB-PLC is a low bandwidth connection where its frequency band is below 500 kHz. Meanwhile BPL uses wider frequency band, range between 2 MHz and 30 MHz [14]. The Figure 2.3 and the Table 2.1 explain the standard for the power line communication frequency bands in Europe. The standard is given according to the CENELEC EN 50065-1. Different frequency band is allocated to different group of users.

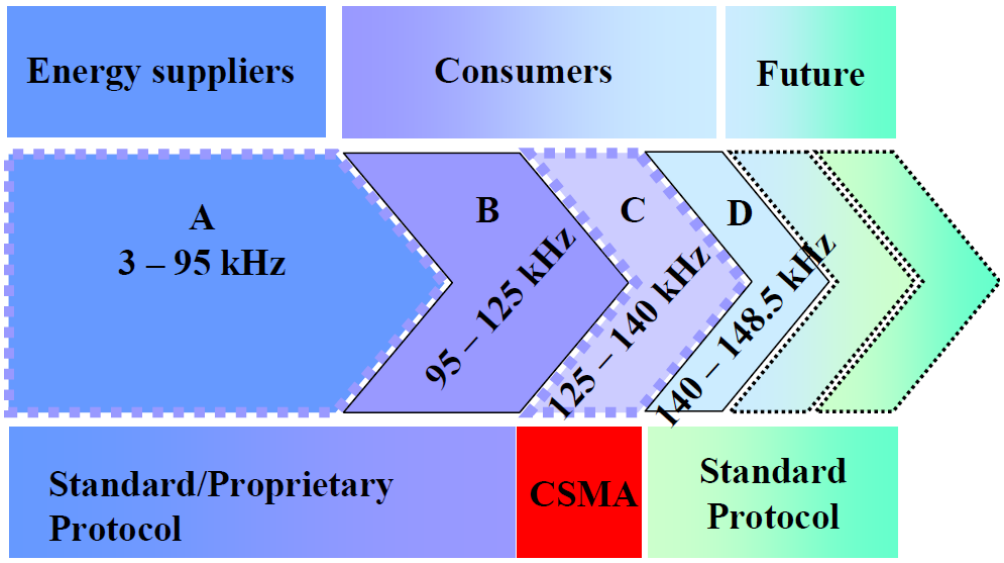

Figure 2.3: The relationship of power line communication frequency bands to different group of users and communication protocols in Europe [15]

Band	Frequency range	Purpose
A	3 kHz – 95 kHz	For electric distribution companies use and their licenses
B	95 kHz – 125 kHz	Available for consumers with no restriction
C	125 kHz – 140 kHz	Available for consumers only with media access protocol
D	140 kHz – 148.5 kHz	Available for consumers with no restriction

Table 2.1: Frequency ranges according to CENELEC EN 50065-1 [16]

In general, the power line communication system is implemented according to the Open System Interconnection (OSI) reference model. Figure 2.4 shows the example of OSI Layers for power line communication. Regardless of the types of modulation used, a power line communication transceiver include a few basic block. Different solutions use numerous level of integration of these components.

Figure 2.5 illustrated the typical block diagram of a power line communication transceiver. Meanwhile the Table 2.2 explained the functions of respective sections in the transceiver.

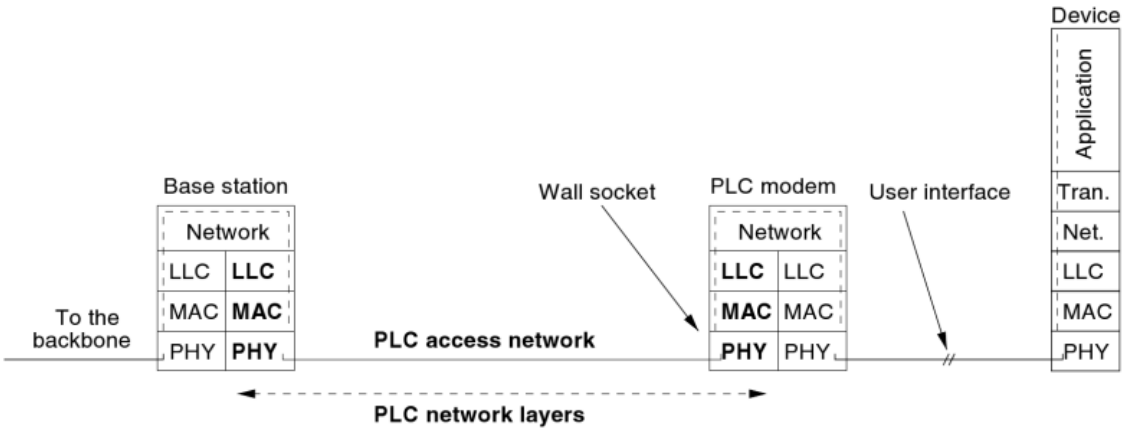

Figure 2.4: Power line specific Open System Interconnection (OSI) Layers [3]

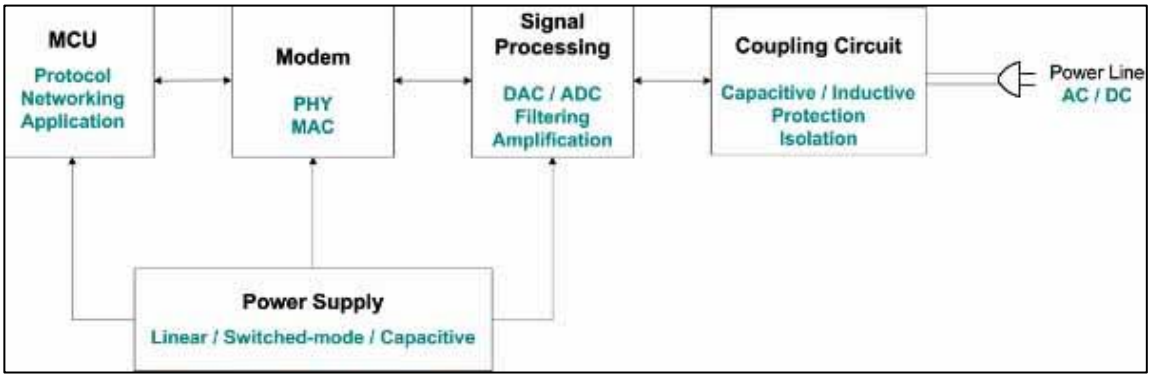

Figure 2.5: Typical block-diagram of power line communication transceiver [17]

Section	Functions
Modem	Core of the transceiver, which is used to implements the Physical and Data Link layers. For example, the modem is responsible to perform modulation – demodulation, error correction and media access control.
MCU	Responsible for networking, protocol, and application-specific functions
Signal Processing	Transmitted and received signals are processed in this section, in digital and analogue form. The main operations include filtering and amplification.
Coupling Circuit	The interface with the power lines is made via a capacitive or inductive coupling circuit, which also provides galvanic isolation and protection against line voltage disturbances. The design of the analogue front-end is related to the channel characteristics, such as amplitude and frequency of

	line voltage, wiring style, location, potential disturbances, applicable regulations, etc.

Table 2.2: List of functions of power line communication transceiver part

2.1.1 NARROWBAND POWER LINE COMMUNICATION

NB-PLC uses the residential electrical power wiring as a transmission medium to control the lighting and electrical appliances without installation of additional new wiring. Typical home control devices operate by modulating in a carrier wave which less than 500kHz in the household wiring from the transmitter [14].The carrier is modulated by digital signals that is generated from the power line communication transceiver, and sending it to another transceiver with the speed up to 200 kbps [14]. Each transceiver in the system has an address and can be individually commanded by the signals transmitted over the household wiring and demodulated at another transceiver. These devices may be either plugged into regular power outlets, or permanently wired in place [3].

NB-PLC systems are mostly based on single-carrier modulation, for instance the modulation technique used are Frequency Shift Keying (FSK), Spread Frequency Shift Keying (S-FSK), Binary Phase Shift Keying (BPSK) and Spread Spectrum (SS). However, the multi-carrier modulation techniques such as Orthogonal Frequency-Division Multiplexing (OFDM) have be used in NB-PLC[14].

The application of the NB-PLC can be implemented provided there is existing electrical wiring in the area. For instance, utility power grid, distributed renewable energy systems to home and buildings, public lighting, and plug-in electric vehicle. There are also others custom applications involving AC, DC or un-powered lines, like fireworks control, emergency lighting and submersible water pumps. [17].

2.2 PROBLEM STATEMENT OF POWER LINE COMMUNICATION

Since power line is not initially designed for communication purposes, it has a few obstacles that will reduce the effectiveness of the signal transmission. In this subchapter, the major problems for power line communication, especially narrowband power line communication will be addressed accordingly, which are high noise level and impedance mismatch. At the same time the solution of these problems will be proposed, and then they will be further explained in the next subchapter.

2.2.1 HIGH NOISE LEVEL

It is pretty common that the high and medium voltage network has channel noise due to lightning, circuit break operations and the transients produced within a power station. In the meantime in low voltage network, the power line communication channel has the highest noise level that is produced from the household machinery and devices and office equipment. In general, the power line in the low voltage network has the strong and time-varying non-white noise. The classification of the noise in the low voltage network is given as following[18]:

(a) Noise Synchronous with the 60 Hz Power Frequency

This type of noise produced from switching devices, such as silicon-controlled rectifier (SCR) and some power supplies. In AC source, an SCR switches at 60 Hz or a multiple of 60 Hz and therefore produced noise at 60 Hz and multiples thereof. This noise is synchronous and drifts with the 60 Hz power frequency. SCR's are abundant part of every power distribution system. This type of noise happens on both the primary and secondary of the distribution line.

(b) Noise with a Smooth Spectrum

This noise is often produced by the loads on the line which do not function synchronously with the power line frequency. A good example is the universal

motor that is implemented in the electrical drill.This type of motor has brushes that make current-switching at intervals which depend on the speed of the motor, where the speed is controlled by the load. For most practical purposes, this noise can be considered as having a smooth spectrum without stationary spectral lines.

(c) Single Event Impulse Noise

Impulse noise is produced from the switching phenomenon, such as lightning and thermostats. The capacitor banks that perform switching-in and out for power-factor correction create impulse noises too.

(d) Nonsynchronous Periodic Noise

This is the noise in which it has line spectra that is not associated with the 60 Hz power frequency. The most typical source of this type of noise is television receivers which produce tones at multiples of the television horizontal scanning line frequency of 15.734 kHz.

Therefore it is crucial to implement a suitable electronic filter to filter out the noise in power line. In this situation, a simple band-pass filter will be sufficient to filter out the noises in narrowband power line communication.

2.2.2 IMPEDANCE MISMATCH

Apart of high noise level, impedance mismatch is another important factor that will affect the data transmission rate in power line communication. The reason is power line has the time-varying and location-varying impedance for both input and output, which will eventually cause the signal to be attenuated [2, 19]. Therefore to ensure the signal can be transmitted correctly, one of the solutions is to increase the signal transmitting power, which results in high energy consumption. In addition to that, there are several negative effects of high power consumption in terms of communication. First, it will cause Electromagnetic Interference (EMI) through emissions which surpass the levels

allowed by regulations. Second, the process wastes more energy. Ultimately, the energy burst will disrupt the other wireless users in adjacent frequency bands [2]. Therefore a better solution to the problem is to match the source impedance and channel impedance at all times, namely impedance matching.

2.3 SOLUTIONS TO THE PROBLEM STATEMENT

This subchapter provides the literature review for band-pass filter and impedance matching. And the review of the relevant research will be included in this subchapter, too.

2.3.1 BAND-PASS FILTER

A band-pass filter allows signals within the specified range of frequencies, namely pass band to pass through and attenuates signals for the frequencies outside this range. Figure 2.6 illustrated the frequency response of a band-pass filter. In power line communication, band-pass filter is required to separate out the unwanted signal such as power line noise at 50 – 60 Hz and the noise at higher frequency, and then allow the communication signal in the kilo-hertz range to pass through the channel[20].

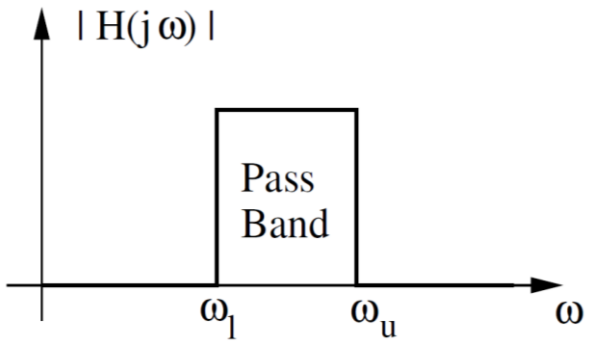

Figure 2.6: Frequency response of band-pass filter

Where

w_l:	Lower cut-off frequency
w_u:	Upper cut-off frequency
$w_0 = \sqrt{w_l w_u}$:	Centre frequency
$B = w_u - w_l$:	Bandwidth
$Q = \frac{w_0}{B}$:	Quality factor

There are various types of band-pass filter in practical application, and one of the simplest types of band-pass filter is RLC band-pass filter, as shown in Figure 2.7.

Another band-pass filter that is newly proposed in this thesis is the LCRC, which will be covered in Chapter 4. Figure 2.8 shows the circuit model of LCRC band-pass filter.

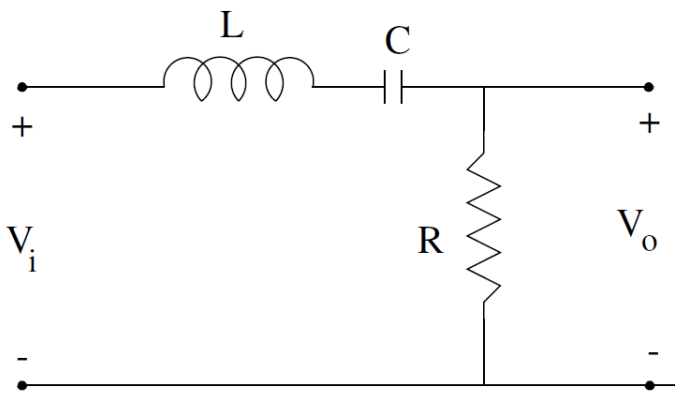

Figure 2.7: RLC band-pass filter circuit diagram

The equation of the transfer function is shown as following:

$$H(jw) = \frac{R}{R + j\left(wL + \frac{1}{wC}\right)} \tag{2.1}$$

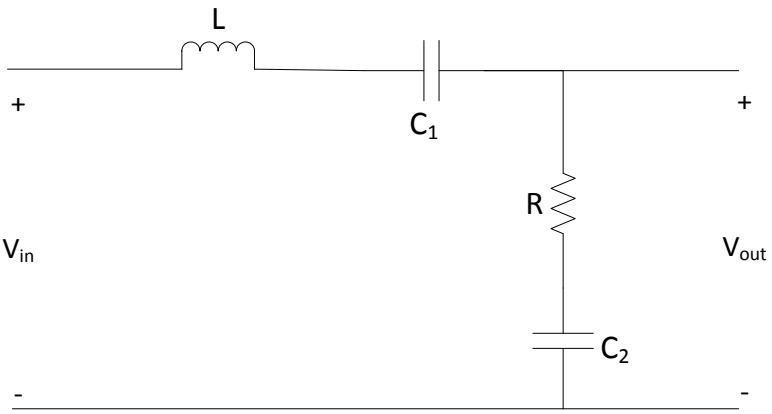

Figure 2.8: LCRC circuit diagram

The transfer function of LCRC is shown below

$$H = \frac{V_{out}}{V_{in}} = \frac{R + \frac{1}{2\pi f C_2}}{R + \frac{1}{2\pi f C_2} + j\left(2\pi f L_1 - \frac{1}{2\pi f C_1}\right)} \tag{2.2}$$

2.3.2 IMPEDANCE MATCHING

Impedance matching is important for communication systems to ensure the maximum power transfer. However, the impedance of a power line is changing depending on time and location, it is rather difficult to achieve matching between the transmitter and the receiver completely in power line communication systems [2, 9, 10, 20]. This is due to the numbers of electrical appliances that are plugged into the networks. Apart of that, the impedance of the channel consists of not only resistance but also reactance which is harmful for high frequency small (low voltage level) signals. Normally, the reactance in power line can be assumed as inductive [10].

The concept of impedance matching is to force a load impedance to become the complex conjugate of the source impedance. In another words the circuit become purely resistive, the load and the source resistance are equal, and net reactance is zero. Therefore the

maximum power can be transferred to the load [21-23]. Not only that, according to Bullock et al, impedance matching will also reduce the radiated power as well as the power line reflection coefficient[7]. For instance, if the source impedance is $Z_s = R + jX$, then its complex conjugate is $Z_s^* = R - jX$. An example of the matching circuit is illustrated in Figure 2.9, in which the reactance value of the load impedance had been cancelled out due to the matching network.

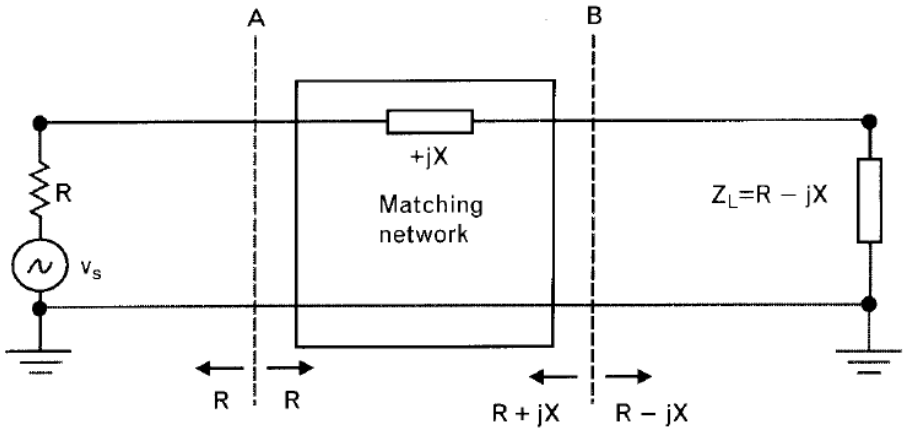

Figure 2.9: Circuit diagram of the matching network concept[22]

In general, there are two types of impedance matching circuit, namely passive impedance matching circuit and adaptive impedance matching circuit. The passive impedance matching circuit consists of electric components, such as fixed tap transformer, resistor, capacitor and inductor. This type of circuit does not perform impedance adaptation, therefore it will only able to match the impedance at the nearest possible value. This offers a cheaper option than the adaptive impedance matching circuit. Meanwhile for adaptive impedance matching circuit, it can perform impedance adaptation to achieve zero net reactance, such as varying the inductance by changing the tap of the coupling transformer in [8], varying the capacitance through the switching of capacitor bank in [9], or even varying the inductance using Voltage Controlled General Impedance Converter (VCGIC) in [10] or Digital Inductive Reactance Converter (DIRC)in [2].Since power line has time and location variable impedance, it is better to use the adaptive impedance matching circuit in order to achieve ideal maximum power transfer in the systems [2, 9, 10].

2.4 IMPEDANCE MEASUREMENT METHOD

In order to achieve the adaptive impedance matching system, it is necessary to have the feedback data, which is the value of the channel impedance. The channel impedance can be measured using the formulation given in [8], where a reference resistor will be needed. The formulation for measurement is based on Figure 2.10.

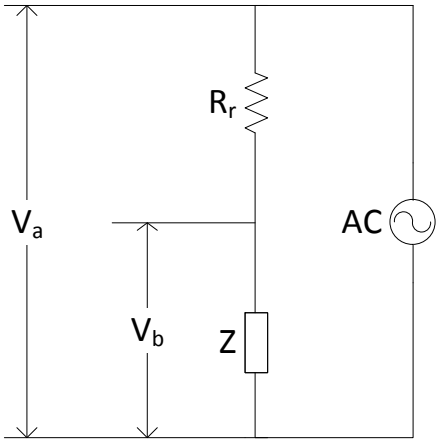

Figure 2.10: Impedance Measurement Circuit Model

Assuming the voltage across reference resistor, R_r, is $V_c = V_a - V_b$. According to [10], the V_a and V_b can be obtained using:

$$V_a = \sqrt{\frac{1}{N}\sum_{i=1}^{N} {x_{ai}}^2 - \frac{1}{N^2}\left(\sum_{i=1}^{N} x_{ai}\right)^2} \tag{2.3}$$

$$V_b = \sqrt{\frac{1}{N}\sum_{i=1}^{N} {x_{bi}}^2 - \frac{1}{N^2}\left(\sum_{i=1}^{N} x_{bi}\right)^2} \tag{2.4}$$

Where x_{ai} and $x_{bi}$are the measured value of V_a and V_b respectively. Higher sampling rate, N yields to better accuracy of V_a and V_b. And then, let $p = \frac{V_a}{V_b}$ and $q = \frac{V_c}{V_b}$, thus

$$X = \frac{(p^2 - q^2 - 1)}{2q^2} R_r \tag{2.5}$$

$$Y^2 = \frac{R_r^2}{q^2} - X^2 \tag{2.6}$$

In this thesis, Equations (2.5)and (2.6) had been further simplified, as shown in Equation(2.7) and (2.8) respectively.

$$X = (p - 1)R_r \tag{2.7}$$

$$Y = \sqrt{\frac{R_r(R_r - q^2)}{q^2}} \tag{2.8}$$

Then, by combining the value X and Y obtained in Equation (2.7)and (2.8), the real and imaginary part of the channel impedance can be obtained as illustrated in Equation (2.9).

$$Z = X + jY \tag{2.9}$$

CHAPTER 3

RLC ADAPTIVE IMPEDANCE MATCHING CIRCUIT

In this chapter, a new circuit model for impedance matching is proposed, in which the concept includes digital capacitor and digital resistor. This circuit model is designed to maximise the matching resolution using simple circuit component. [24]

3.1 CIRCUIT MODEL

A simplified circuit diagram of a RLC band-pass filter adaptive impedance matching circuit is shown in Figure 3.1. The circuit consists of three parts: the differential signal generator and the source impedance, the RLC band-pass adaptive impedance matching circuit and the power line channel impedance or load impedance. The impedance matching process occurs when the middle part of the circuit is operating to match both the left (source impedance) and the right (channel impedance) hand sides of the circuit. This concept works by varying the value of the digital capacitor and digital resistor which controlled by a microcontroller. These values depend on the feedback value from the measured source impedance and channel impedance.

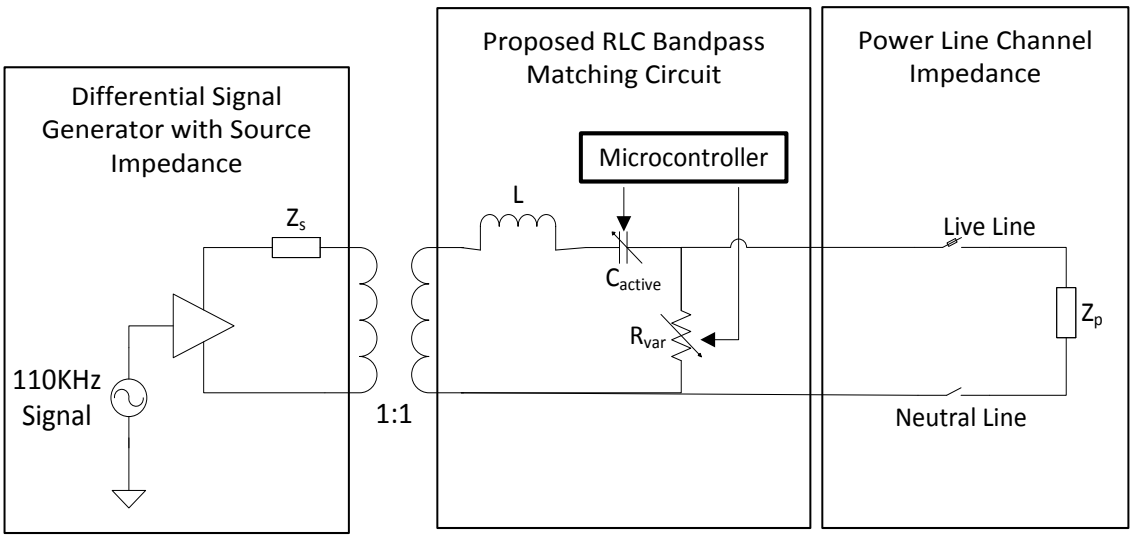

Figure 3.1: Proposed RLC band-pass filter impedance matching circuit

The RLC band-pass filter circuit model is proposed in this chapter as its component can be altered easily, and it can filtered out the noise, allows only the power line modulated frequency to pass through the communication channel.

3.2 DIGITAL CAPACITOR

The digital capacitor is used as the variable capacitor that can be controlled through microcontroller. This concept is proposed in [25]. The digital capacitor works using binary systems, therefore higher bits yields to higher resolution. Figure 3.2 illustrates the example of the digital capacitor, which is a 4 bits system, ranging from 1 nF to 15 nF. For instance, in order to achieve the value of 12 nF, the value 12 in decimal need to be converted into binary, as shown in Equation (3.1).

$$12_{10} = 1100_2 \tag{3.1}$$

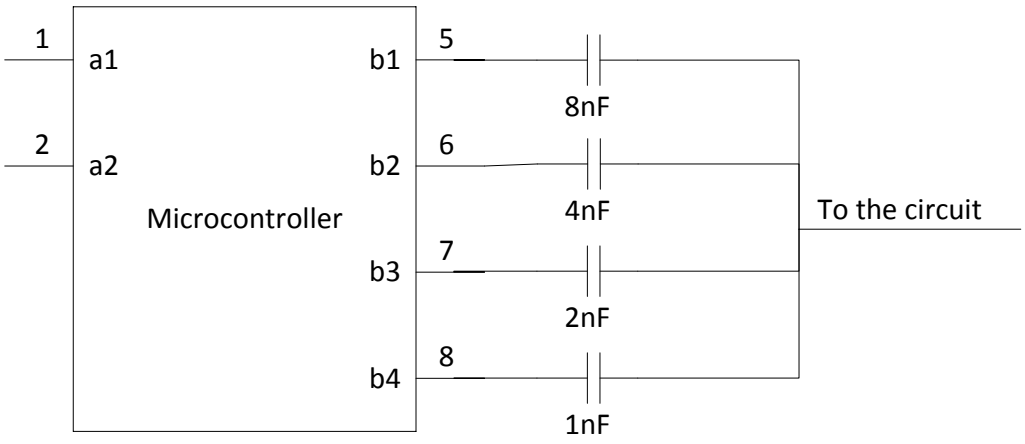

Figure 3.2: 1-15nF 4 bit digital capacitor

Then from 1100_2 binary number, the switch 5 and 6 will turn on, and then the capacitive value of 12 nF will be:

$$2^3 + 2^2 = 8 + 4 = 12\ nF \tag{3.2}$$

In this chapter, the 1-63 nF 6 bit digital capacitor is used to perform impedance matching.

3.3 IMPEDANCE MATCHING ALGORITHM

Figure 3.3 illustrates the circuit model of the RLC band-pass impedance matching circuit. There are two types of impedance used in the calculation, which are the source impedance, Z_s and the channel impedance, Z_p. These variables are measured value in the power line. Therefore it will vary according to the status of the connected load.

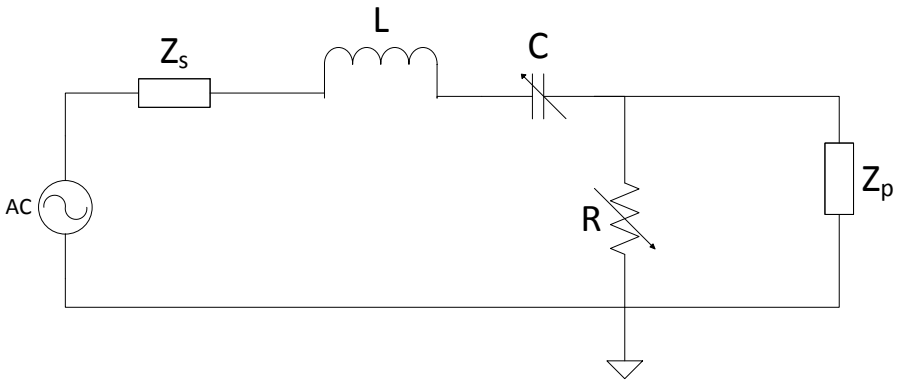

Figure 3.3: Proposed RLC band-pass filter impedance matching circuit model

Assuming that Z_s and $Z_p$consist of real part only, the following method can be used to find R and C.

Let $X = X_L - X_C$

$$Z_s = jX + \frac{RZ_p}{R + Z_p} = \frac{jX(R + Z_p) + RZ_p}{R + Z_p} \tag{3.3}$$

$$Z_p = \frac{(Z_s + jX)R}{R + Z_s + jX} = \frac{RZ_s + jXR}{R + Z_s + jX} \tag{3.4}$$

Simplify Equation (3.3) to Equation (3.5), and Equation (3.4) to Equation (3.6), therefore:

$$RZ_s + Z_sZ_p = RZ_p + jXR + jXZ_p \tag{3.5}$$

$$RZ_p + Z_sZ_p + jXZ_p = RZ_s + jXR \tag{3.6}$$

Combine Equation (3.5) and Equation (3.6) yields,

$$Z_s Z_p = jXR \tag{3.7}$$

Rearrange Equation (3.7) to become

$$X = \frac{Z_s Z_p}{jR} \tag{3.8}$$

Substitute Equation (3.8) into Equation (3.6)

$$RZ_p + Z_s Z_p + j\left(\frac{Z_s Z_p}{jR}\right) Z_p = RZ_s + j\left(\frac{Z_s Z_p}{jR}\right) R \tag{3.9}$$

Rearrange Equation (3.9) to become

$$R^2 = \frac{Z_s {Z_p}^2}{Z_p - Z_s} \tag{3.10}$$

The digital capacitor C can be calculated by $X_c = X - X_L$, where

$$C = \frac{1}{2\pi f X_c} \tag{3.11}$$

Also, R is obtained from Equation (3.10). The value obtained from Equation (3.10) and (3.11) will compare with the original value of R and C, and then adjust the value if it is different from the calculated value. Note that Equation (3.8) and (3.10) are only valid if Z_p is greater thanZ_s, because R has to be positive value all the time.

In order to clarify the error of the calculation, the value obtained from Equation (3.10) and (3.11) are substituted back into Equation (3.3) and (3.4) and then the calculated Z_s and Z_p have been compared with the existing value using Equation (3.12), as shown below.

$$error = \frac{|Z_{measured} - Z_{calculated}|}{Z_{measured}} \times 100\% \quad (3.12)$$

By using MATLAB, the simulated result shows that the error is 0% or a negligible small value. Therefore this method is applicable to find the value of R and C.

3.4 EXPERIMENTS

This subchapter covers about the methods used to verify the concept. In general, the concept can be tested through theoretical analysis and practical analysis. The theoretical analysis used in this subchapter is software simulation using PSIM and MATLAB. PSIM stands for power simulation software, which is used to design the power electronics and motor control. Meanwhile the practical analysis used in this subchapter is to perform the experimental analysis by constructing the circuit model using the electronic components in the laboratory.

3.4.1 SIMULATION RESULT

In order to verify the feasibility of the concept, the simulation had been performed using MATLAB and PSIM. The concept had been tested with both minimum load and maximum load. Table 3.1 tabulated the value of the source impedance and channel impedance during minimum load and maximum load. The impedance value was taken according to the measured value in [26]. Through many trial and error of the simulation, it was decided that L = 5 μH inductor was used in this paper to ensure the centre frequency is in the range of 110 kHz. The 50 Ω resistor is connected in series with the Z_p to prevent the Z_p greater than Z_s.

Load type	Source Impedance, Z_s (Ω)	Channel Impedance, Z_p(Ω)
Min. Load	15	5(total 55)
Max. Load	15	250(total 300)

Table 3.1: Minimum and maximum source and channel impedance

Table 3.2shows the resistance and capacitance value of the circuit, in which they can be calculated using Equation (3.8), (3.10)and (3.11).

Load type	Resistance, R (Ω)	Capacitance C (nF)
Min. Load	34	58
Max. Load	69	22

Table 3.2: Calculated resistance and capacitance value

Figure 3.4 illustrated the circuit diagram of the RLC band-pass filter impedance matching circuit, drawn using PSIM. Meanwhile Figure 3.5 and Figure 3.6 are the simulated curve for voltages and currents. Note that V_{in} = 10 V peak.

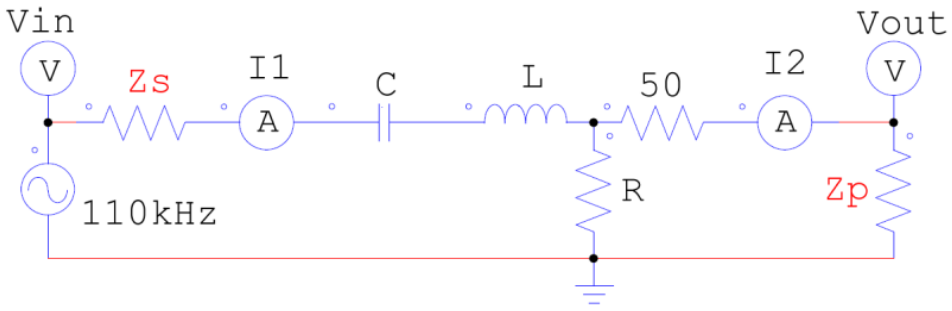

Figure 3.4: PSIM drawing of RLC band-pass filter impedance matching circuit

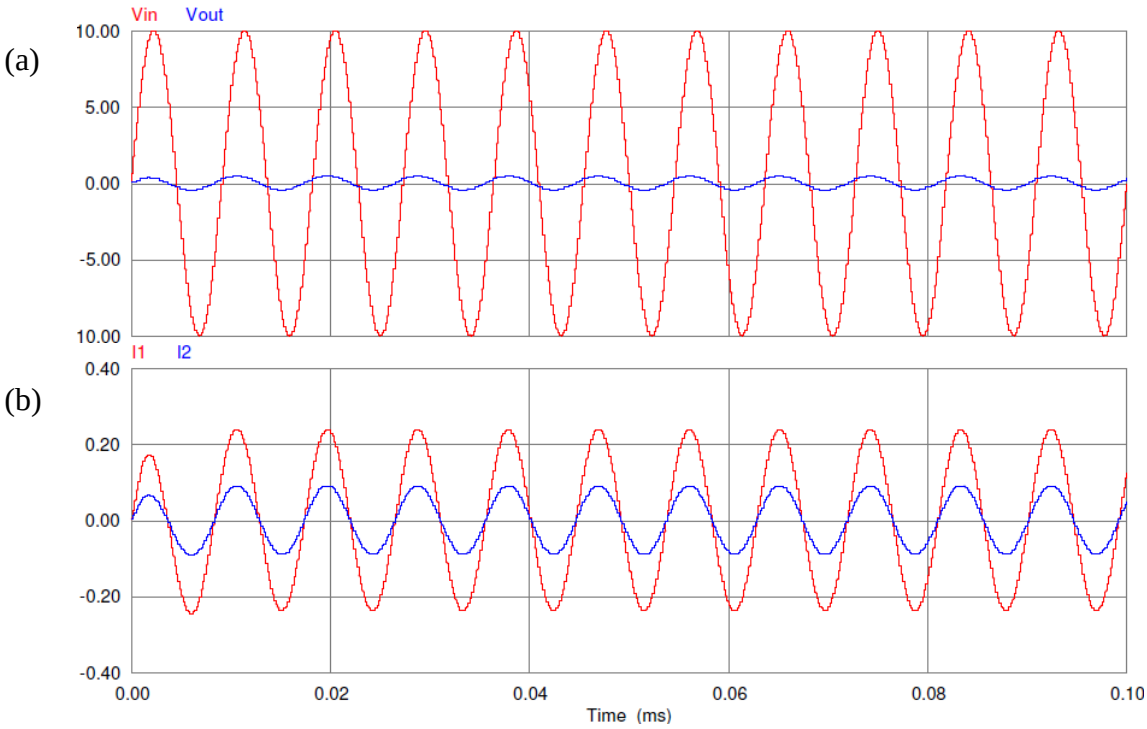

Figure 3.5: PSIM simulation for (a) voltage and (b) current waveform for minimum load respectively

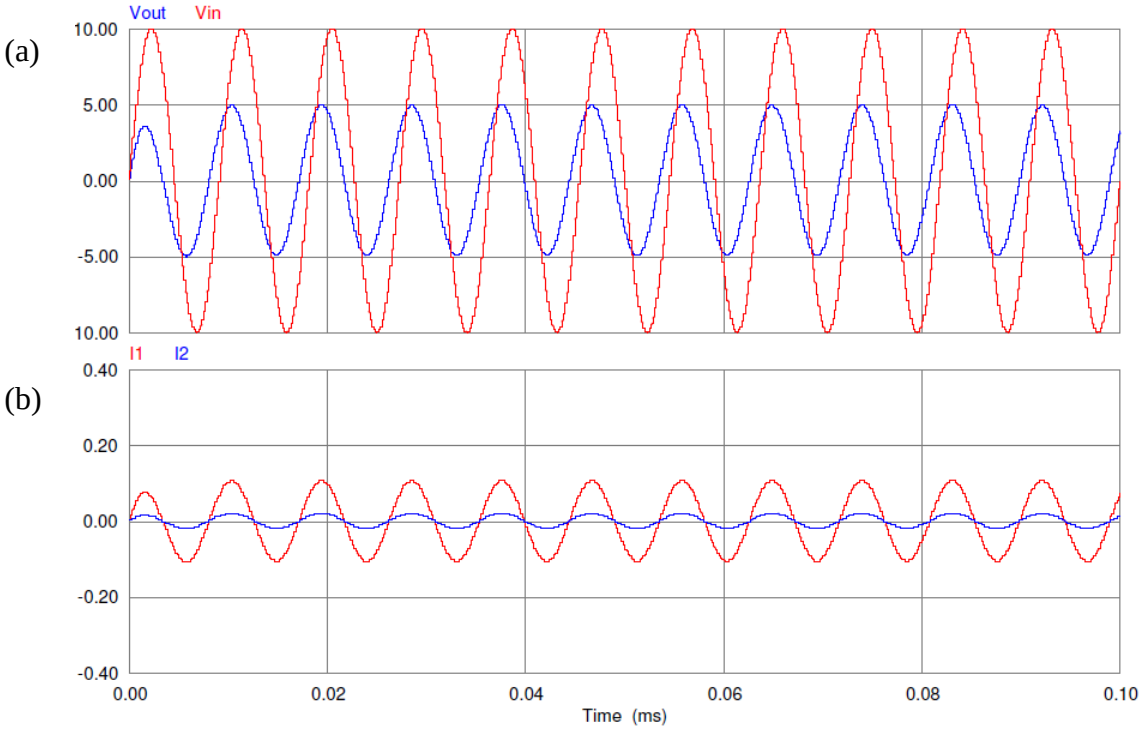

Figure 3.6: PSIM simulation for (a) voltage and (b) current waveform for maximum load respectively

From Figure 3.5 and Figure 3.6, the output voltage, V_{out} and output current, I_2 are varying depending on the types of load connected to the channel impedance. In Figure 3.6, it is clearly shows that the V_{out} is half of the input voltage, V_{in}, which proves that the maximum power transfer is achieved in the system.

It is crucial to verify whether the modulated frequency signal can pass through the matching circuit. This can be tested using MATLAB. By using the values in Table 3.2, the magnitude versus frequency curve had been drawn in Figure 3.7 and Figure 3.8 for minimum and maximum load. The magnitude of the curve is calculated using the transfer function of the circuit, which is displayed in Equation (2.1).

From the Figure 3.7 and Figure 3.8, they clearly show that the centre frequency is around 110 kHz, and the bandwidth is sufficient for the modulated frequency to pass through. Therefore this impedance matching concept is feasible in the application of power line communication.

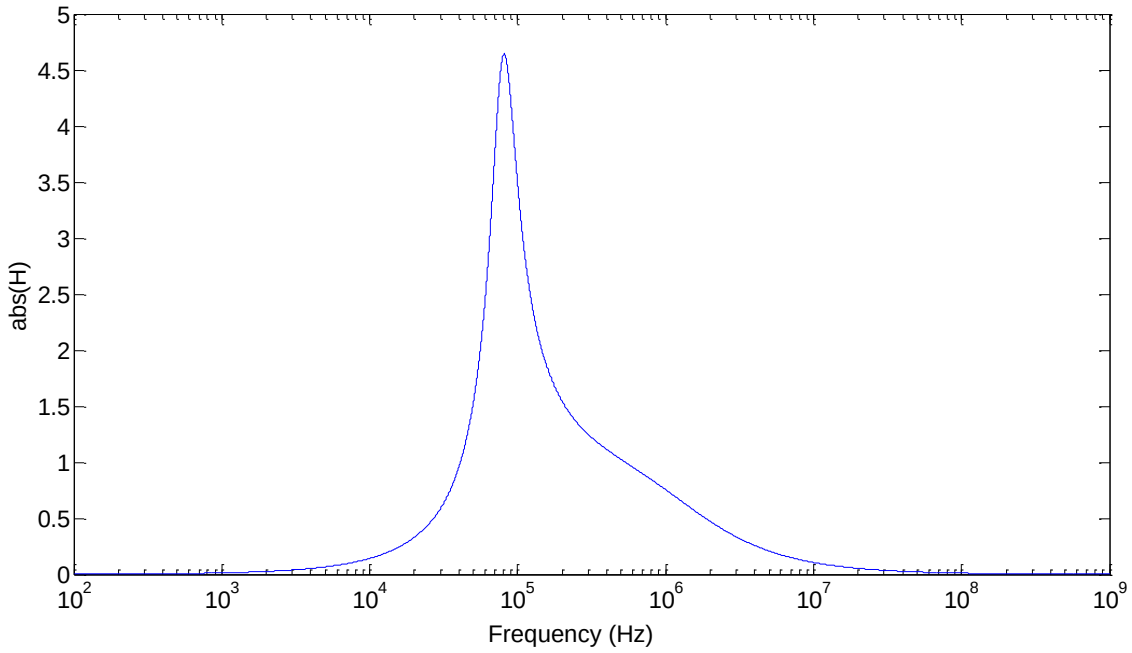

Figure 3.7: MATLAB simulation for magnitude plot of the circuit in minimum load

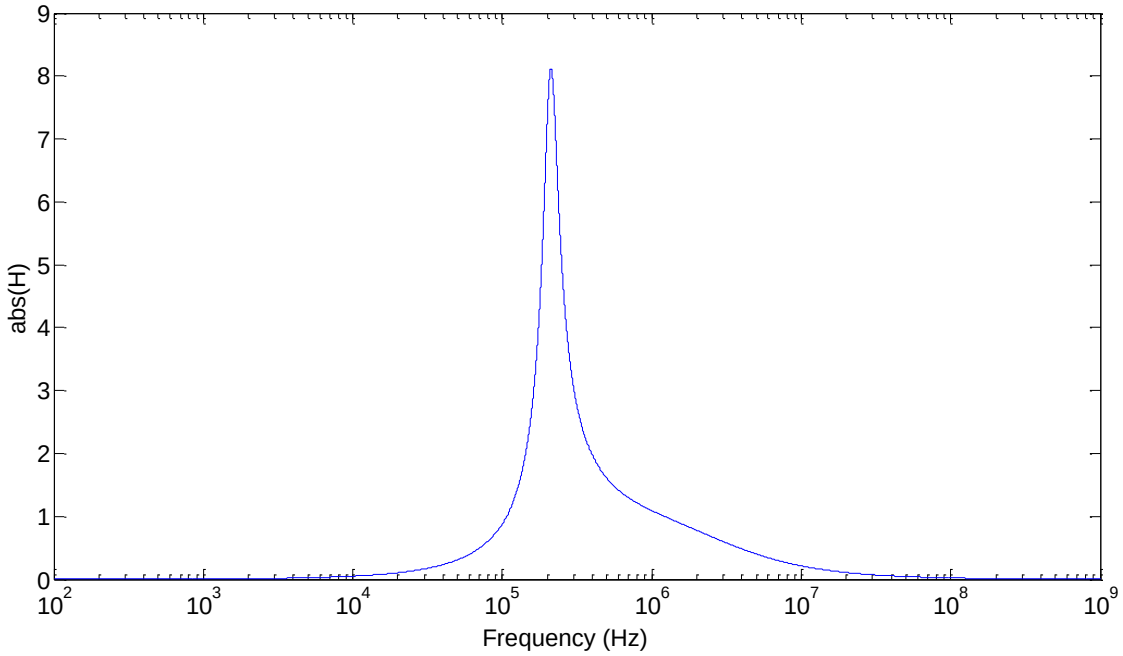

Figure 3.8: MATLAB simulation for magnitude plot of the circuit in maximum load

From the simulated result, it is clearly shows that this methodology is applicable in the NB-PLC channel.

3.4.2 MEASURED RESULT

After the simulation verification had been completed, the next step is to verify the concept through practical analysis. The circuit diagram shown in Figure 3.4 had been constructed using the electronic components that are available in the laboratory. For laboratory verification purpose, the decade resistance box and capacitance box is used to substitute the digital resistor and digital capacitor respectively. And then, function generator is used to act as the voltage source and also the source of the modulated frequency. Meanwhile, the oscilloscope is used as the tool to measure the voltage and current waveform at both input and output side of the circuit.

The parameter of this experiment is identical to the parameters set in the PSIM simulation. So the input voltage is remaining as 10 V peak to peak, the generated

frequency is 110 kHz and the value of L is close to 5μH. And the rest of the given parameters are similar to Table 3.1 and Table 3.2. After that, compare the measured result with the theoretical analysis to find out the feasibility of the concept in practical situation.

Note that the oscilloscope in the laboratory can only be used to measure the voltage. So it is necessary to use differential current probe to measure the current. The range of the current probe used in this experiment is 100 mV/A.

From the Figure 3.9, Figure 3.10, Figure 3.11 and Figure 3.12, the measured results are comparable to the simulated result in Figure 3.5 and Figure 3.6. Then from Figure 3.11, it is clearly shown that the output voltage is half of the input voltage. So the maximum power transfer can be observed from this experiment. Therefore this impedance matching circuit is practical to be used in the actual application to reduce the noise level and also reduce the impedance mismatch in the power line communication system. This methodology can also be used in wireless communication system, but different configuration of the components may be required to achieve maximum power transfer in the system. The developed impedance matching circuit is limited to narrowband communication only.

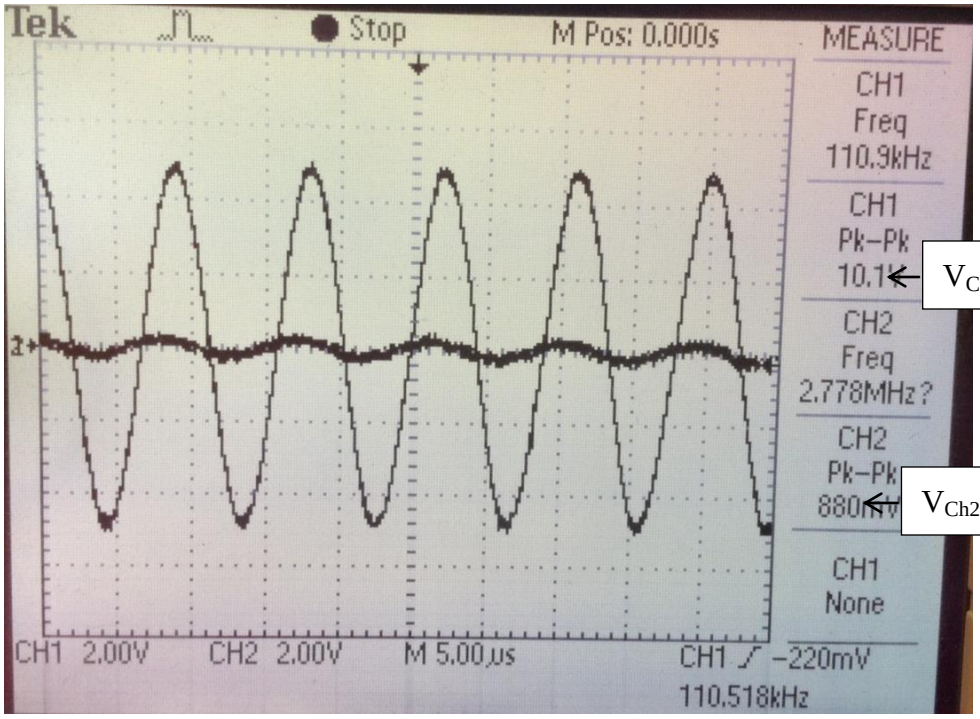

Figure 3.9: Oscilloscope measurement for voltage waveform at minimum load

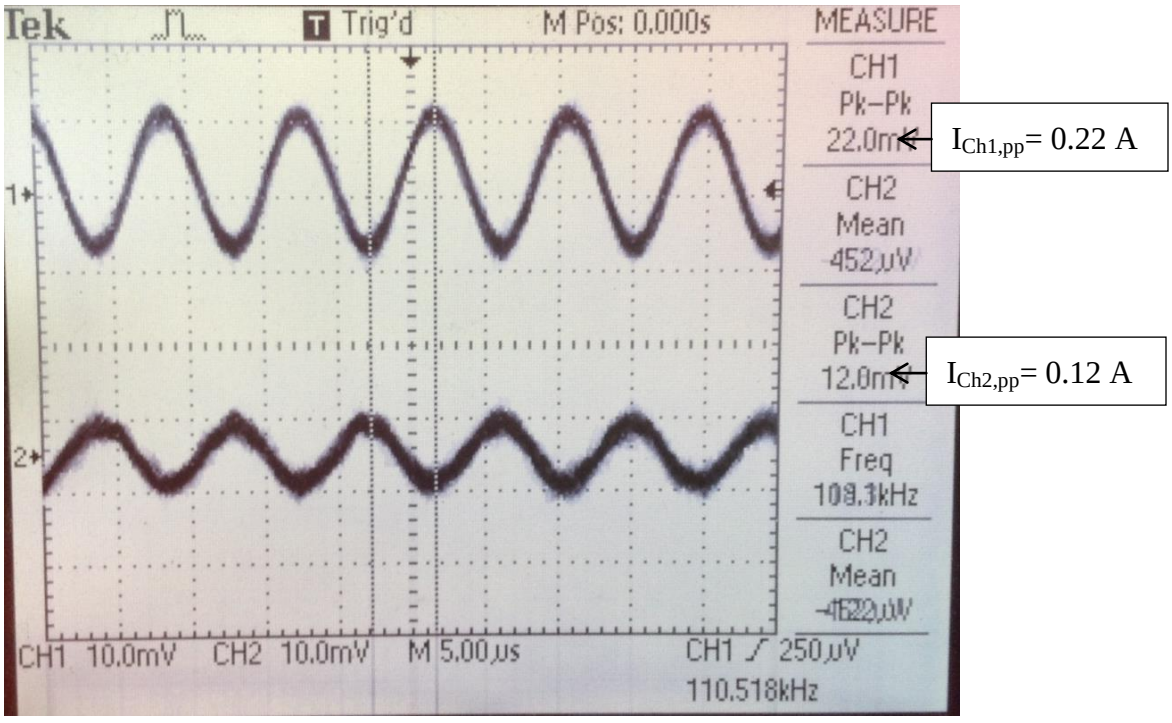

Figure 3.10: Oscilloscope measurement for current waveform at minimum load (100 mV = 1 A)

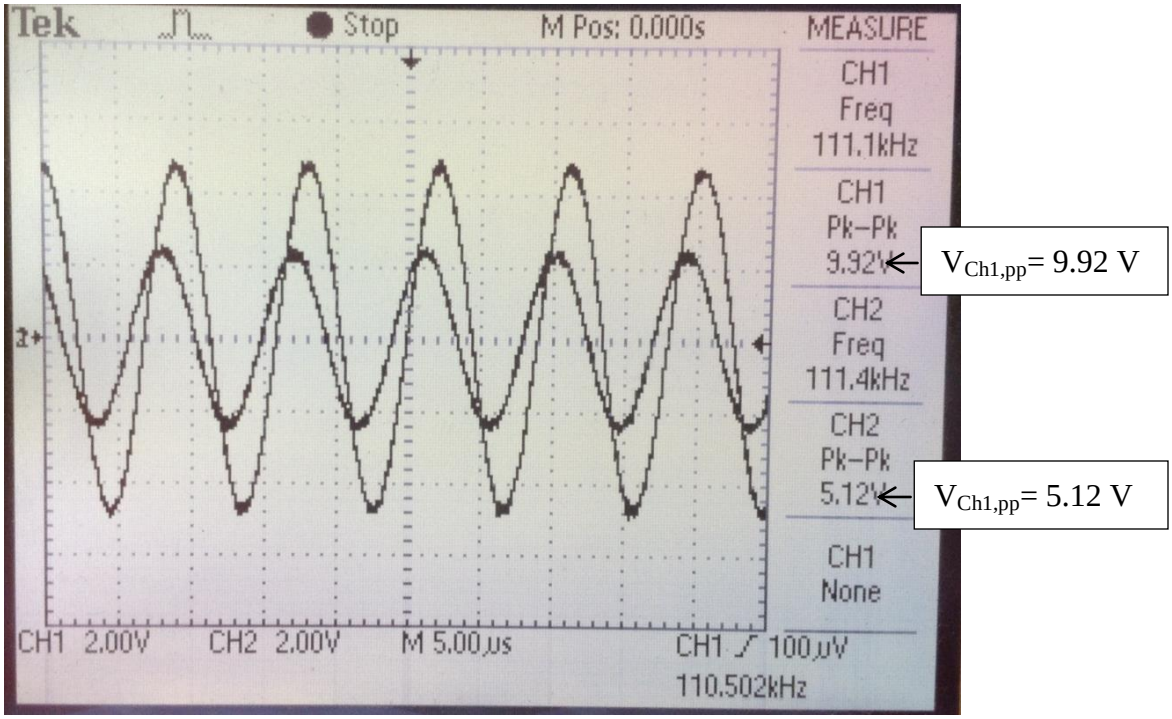

Figure 3.11: Oscilloscope measurement for voltage waveform at maximum load

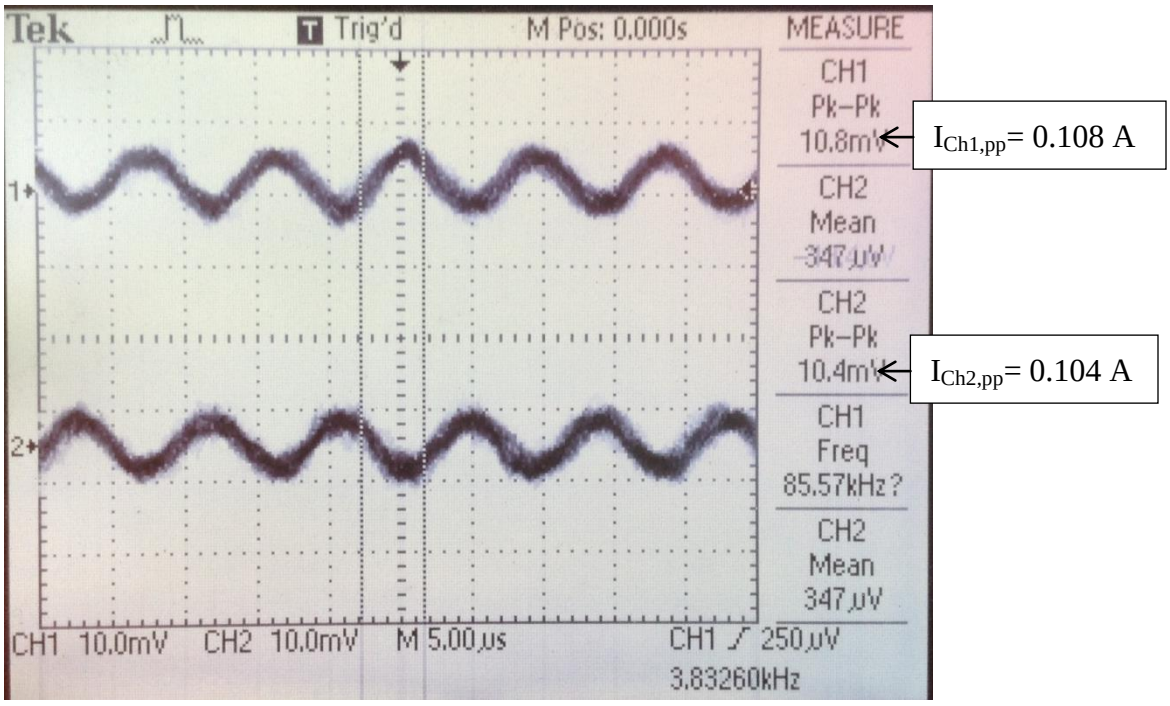

Figure 3.12: Oscilloscope measurement for current waveform at maximum load (100 mV = 1 A)

3.5 SUMMARY

This chapter proposed a new methodology of impedance matching in NB-PLC channel. This method has relatively simple and clear mathematic algorithm to match the power line communication source and channel impedances continuously. Therefore maximum power transfer can be achieved. By comparing with other existing adaptive impedance matching method, this method has advantage in higher matching resolution and easier control. This method is tested and verified through PSIM and MATLAB simulation, and it had also been tested in the laboratory to ensure it is feasible to use in the actual application of NB-PLC, in order to reduce noise level and impedance mismatch.

CHAPTER 4

LCRC ADAPTIVE IMPEDANCE MATCHING CIRCUIT

In this chapter, the improved matching circuit of Chapter 3 was proposed. This impedance matching circuit model has an additional digital capacitor in series with the digital resistor, and then a fixed inductor had been changed to an active inductor instead. Therefore this circuit model is named as LCRC adaptive impedance matching circuit model. It was designed to improve the matching resolution when the source and channel impedance includes reactive components using simple circuit component. In addition to that, it has the advantage of ensuring the bandwidth being narrow.

4.1 CIRCUIT MODEL

A PLC circuit diagram of a LCRC adaptive impedance matching circuit is shown in Figure 4.1. Similar to the RLC circuit based PLC model in Chapter 3, it is divided into three parts. The left hand side part consists of a differential signal generator its source impedance. The middle part is the proposed LCRC adaptive impedance matching circuit. Meanwhile the right hand side part is the power line channel impedance or load impedance. The impedance matching process occurs when the middle part of the circuit is operating to match the source impedance to the channel impedance of the circuit. This concept works by varying the value of the active inductor L, digital capacitor C_1 and C_2 and digital resistor R_{var}through a microcontroller. These values are obtained by comparing the measured source impedance to the measured channel impedance.

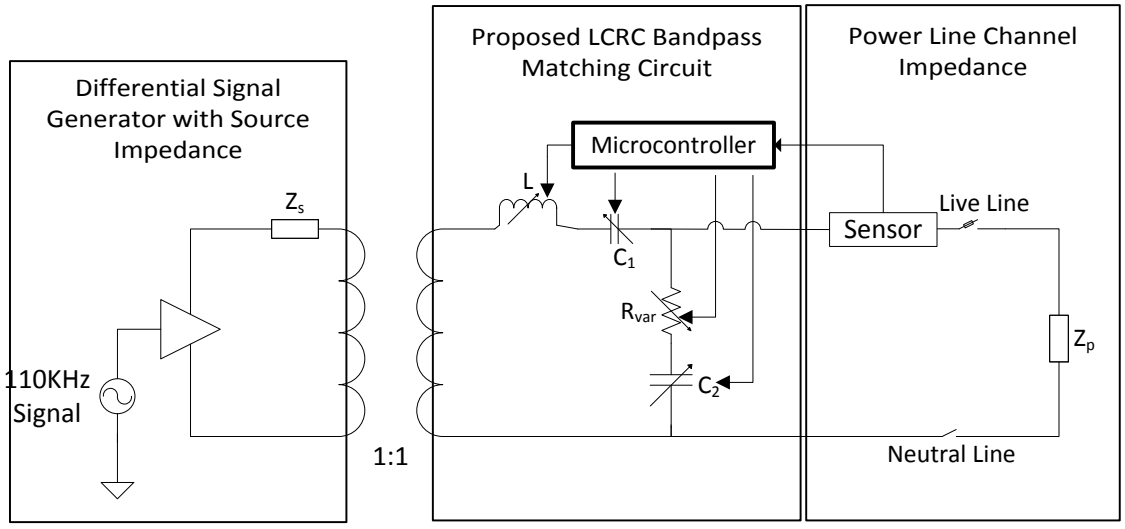

Figure 4.1: PLC with aLCRC Adaptive Impedance Matching Circuit

The LCRC circuit model is better than the RLC circuit model in Chapter 3 because the calculation includes the reactance of the source and load impedance. And then the concept includes the calculation that will ensure the circuit has narrowband bandwidth.

4.2 ACTIVE INDUCTOR

The active inductor mentioned in this chapter is achieved by using the Antonius's General Impedance Converter (GIC) [27, 28]. The schematic of the GIC is demonstrated in Figure 4.2. The input impedance of this structure is obtained by Equation (4.1)

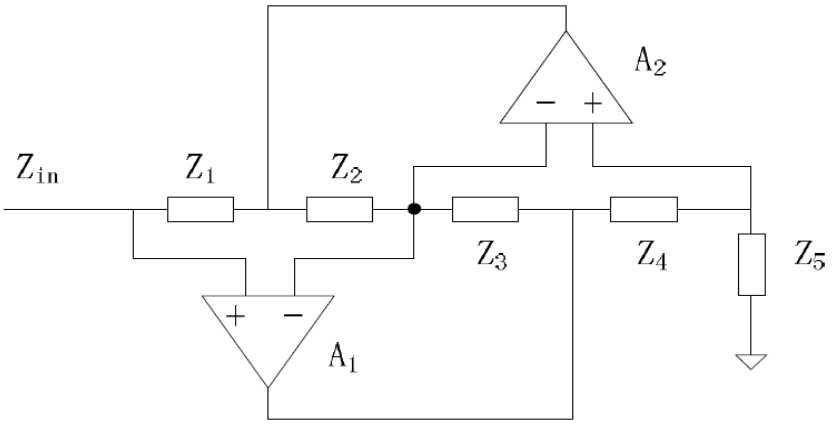

Figure 4.2: General Impedance Converter (GIC)[2]

$$Z_{in} = \frac{Z_1 Z_3 Z_5}{Z_2 Z_4} \tag{4.1}$$

In order to achieve inductive reactance, one of the components in denominator has to be a capacitor and the others are resistors. Figure 4.3 shows the circuit diagram of the active inductor. So the new input impedance can be written as shown in Equation (4.2) [29].

$$Z_{in} = \frac{sCR_1R_3R_5}{R_2} \tag{4.2}$$

And then through inspection, the value of the inductor in this case can be calculated by using Equation (4.3) [29].

$$L = \frac{CR_1R_3R_5}{R_2} \tag{4.3}$$

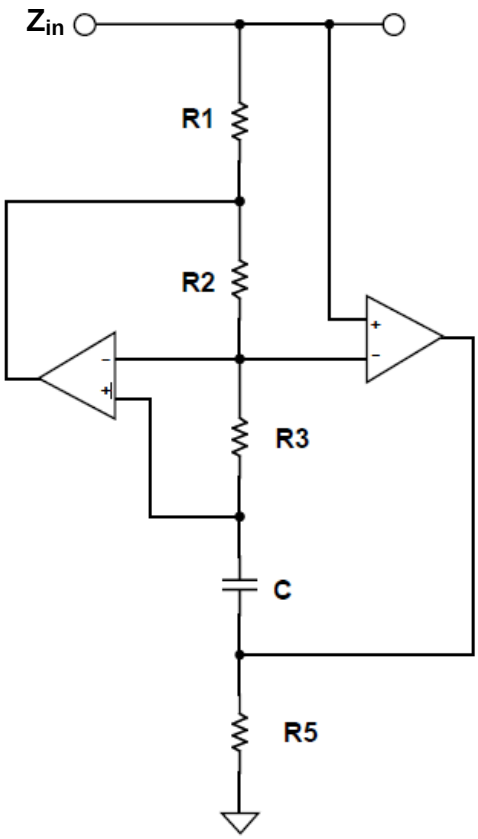

Figure 4.3: Active Inductor[29]

In order to adjust the value of the inductance, R1, R_3 or R_5 can be replaced to become a digital resistor.

4.3 IMPEDANCE MATCHING ALGORITHM

Figure 4.4 illustrated a PLC circuit model with a LCRC impedance matching circuit. The circuit shown in Figure 4.4 is similar to the circuit used in Chapter 3, with the only difference being the addition of a real and imaginary part, and the exchange from a fixed inductor to an active inductor. Therefore the circuit model resembles the actual application of PLC, where both the source and load impedance consists of both resistance and reactance.

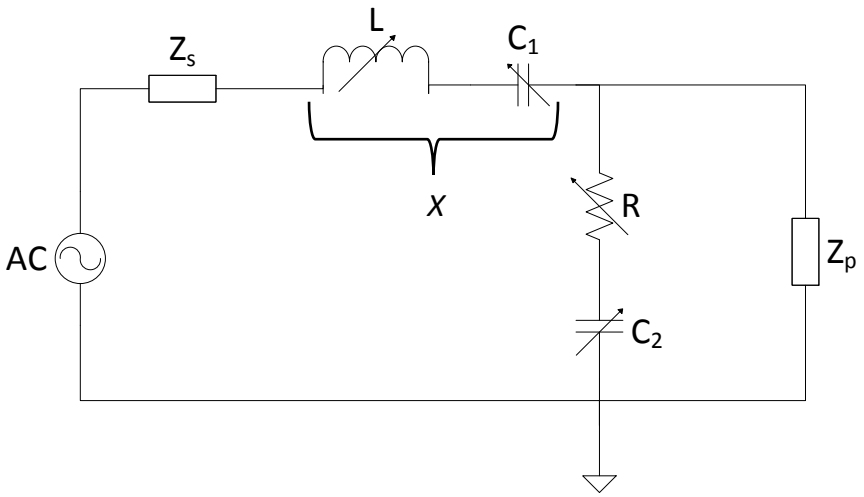

Figure 4.4: Simplified PLC circuit model with aLCRC Impedance Matching system

The source impedance, Z_s is comes from the computer, so it is fixed value. Meanwhile the channel impedance, Z_p is depending on electrical appliances. Therefore, it is crucial to have a feasible LCRC impedance matching network to match the load impedance to the source impedance. In other words, it is necessary to verify whether the design allows the matching filter to be adaptive according to Z_p and Z_s as well as fulfil the frequency and transient response requirement. Therefore, the core parameter of the filter is required to be established. L is chosen to be the key parameter of the filter since its value determines the filter specification. It implies that other parameters such as R, C_1 and C_2 are functions of L.

4.3.1 MATHEMATICAL DERIVATION TO FIND R, C_1 AND C_2

In order to perform the impedance matching using the LCRC circuit model, the first step is to derive the equations that are able to express the relationship between the R, C1 and C2, and Z_p and Z_s. Since the LCRC circuit are not much different from the RLC circuit model, the equations listed in Chapter 3 can be reapplied and modified to achieve this purpose. So, let X_{C_2} to be expressed as follow:

$$X_{C_2} = \frac{1}{2\pi f C_2} \tag{4.4}$$

Note that$X_{C_2} < 0$ because it refers to the capacitive reactance. Meanwhile, Z_2 represents the total impedance for R and C_2, as written below:

$$Z_2 = R - jX_{C_2} \tag{4.5}$$

Assuming that the central frequency, $f_0$is 3kHz and $Z_p$has imaginary part that is $Z_p \in \mathbb{C}$. Then Equation (4.5) is substituted into Equation (3.8) and Equation (3.10) from Chapter 3to become Equation (4.6) and Equation (4.7) respectively.

$$X = \left|\frac{Z_s Z_p}{Z_2}\right| \tag{4.6}$$

$$Z_2 = R + jX_{C_2} = \sqrt{\frac{Z_s {Z_p}^2}{Z_p - Z_s}} \tag{4.7}$$

So Equation (4.6) and Equation (4.7) acts as the fundamental formulas to solve for R, C_1 and C_2.

4.3.2 MATHEMATICAL DERIVATION TO FORM RELATIONSHIP BETWEEN R AND L

In order to ensure the narrowband bandwidth of the circuit, the value of L will become the crucial parameter to control the bandwidth. Therefore, the following method is applied to find L. The transfer function of LCRC is given in Equation (2.2).

Let C_1 to be written as following:

$$C_1 = \frac{1}{2\pi f_0 (X_L - X)} \tag{4.8}$$

As a result,

$$\frac{1}{2\pi f C_1} = \frac{1}{2\pi f \left(\frac{1}{2\pi f_0 (X_L - X)}\right)} = \frac{f_0}{f}(X_L - X) \tag{4.9}$$

Substitute the result of Equation (4.9) into Equation (2.2) to form Equation (4.10)

$$H = \frac{Z_2}{Z_2 + j\left(2\pi f L - \frac{f_0}{f}(X_L - X)\right)} \tag{4.10}$$

Then, the magnitude of the transfer function is shown in Equation (4.11)

$$|H| = \frac{\sqrt{R^2 + {X_{C_2}}^2}}{\sqrt{R^2 + \left(2\pi f L - \frac{f_0}{f}(X_L - X_c) - X_{C_2}\right)^2}} \tag{4.11}$$

Mathematically, the maximum or minimum point of the curve is attained when the differentiation for the magnitude of the transfer function is equal to zero, as shown in the following equation;

$$|H_{max}| = \frac{d|H|}{df} = 0$$

So the differentiation of Equation (4.11) is obtained as shown below

$$\frac{d|H|}{df} = \frac{\left(-2\pi L + \frac{f_0}{f^2}(X_L - X)\right)\sqrt{{R_2}^2 + {X_2}^2}\left(2\pi fL - \frac{f_0}{f}(X_L - X) - X_{C_2}\right)}{\left(R^2 + \left(2\pi fL - \frac{f}{f_0}(X_L - X) - X_{C_2}\right)^2\right)^{\frac{3}{2}}} \quad (4.12)$$

Since f_0 is the maximum point in the curve,

$$\left.\frac{d|H|}{df}\right|_{f=3000\ Hz} = 0$$

Therefore from Equation (4.12), it can be further simplified to

$$\left(-2\pi L + \frac{f_0}{f^2}(X_L - X)\right)\left(2\pi fL - \frac{f_0}{f}(X_L - X) - X_{C_2}\right) = 0$$

Then it can be written separately into Equation (4.13)and Equation (4.14)

$$\left.-2\pi L + \frac{f_0}{f^2}(X_L - X)\right|_{f=3000\ Hz} = 0 \quad (4.13)$$

$$\left.2\pi fL - \frac{f_0}{f}(X_L - X) - X_{C_2}\right|_{f=3000\ Hz} = 0 \quad (4.14)$$

In order to find X, it is necessary to solve Equation (4.13)and Equation (4.14) respectively. From Equation (4.13), it can be rearranged to become Equation (4.15).

$$2\pi fL - X = 2\pi L\frac{f^2}{f_0} \tag{4.15}$$

After that substitute the $f = f_0 = 3000\ Hz$ into Equation (4.15) to find the solution for X.

$$X = 2\pi(3000)L + 2\pi\frac{(3000)^2}{3000}L = 0$$

Notice that $X = 0$ in this case. Since this solution is for minimum point of the curve, therefore it can be neglected. Then from Equation (4.14), it can be rearranged to become

$$\frac{f_0}{f}(2\pi fL - X) = 2\pi fL - \frac{1}{2\pi fC_2} \tag{4.16}$$

Again, substitute the $f = f_0 = 3000\ Hz$ into Equation (4.16) to find X.

$$\frac{3000}{3000}(2\pi \times 3000 \times L - X) = 2\pi \times 3000 \times L - \frac{1}{2\pi \times 3000 \times C_2}$$

So, the solution of$X$ is calculated as

$$X = \frac{1}{6000\pi C_2} \tag{4.17}$$

Thus, Equation (4.17) can be used to express the relationship between$X$ andC_2. In order to design the band-pass filter with $f_0 = 3000$ Hz, substitute both f and f_0 = 3000 Hz into Equation (4.11), as shown in Equation (4.18).

$$|H| = \left. \frac{\sqrt{R^2 + {X_{C_2}}^2}}{\sqrt{R^2 + \left(2\pi fL - \frac{f_0}{f}(X_L - X_c) - X_{C_2}\right)^2}} \right|_{f=f_0=3000\ Hz} \tag{4.18}$$

Rearrange Equation (4.18) to become Equation (4.19)

$$|H| = \left. \frac{\sqrt{R^2 + {X_{C_2}}^2}}{\sqrt{R^2 + \left(2\pi(f - f_0)L + \frac{f_0}{f}X - X_{C_2}\right)^2}} \right|_{f=f_0=3000\ Hz} \tag{4.19}$$

$$|H|\big|_{f=3000\ Hz} = \frac{\sqrt{R^2 + {X_{C_2}}^2}}{\sqrt{R^2 + \left(2\pi(3000 - 3000)L + \frac{3000}{3000}X - X_{C_2}\right)^2}}$$

Simplify the equation above to become Equation (4.20)

$$|H|\big|_{f=3000\ Hz} = \frac{\sqrt{R^2 + {X_{C_2}}^2}}{\sqrt{R^2 + \left(X - X_{C_2}\right)^2}} \tag{4.20}$$

And then expand the $X$and X_{C2}, as illustrated in Equation (4.21)

$$|H|\big|_{f=3000\ Hz} = \frac{\sqrt{R^2 + {X_{C_2}}^2}}{\sqrt{R^2 + \left(\frac{1}{6000\pi C_2} - \frac{1}{6000\pi C_1}\right)^2}} \tag{4.21}$$

In order to simplify the calculation, let $C_1 = C_2$. Therefore Equation (4.21)can be further simplified to

$$|H|_{max} = \frac{\sqrt{R^2 + {X_{C_2}}^2}}{R} \tag{4.22}$$

Another criterion that needs to be taken into account in the filter design is the narrowband bandwidth of the filter. Usually the bandwidth for the narrowband band-pass filter is 1000 Hz. Therefore the lower and upper cut-off frequency is set to be 2500 Hz and 3500 Hz respectively.

At lower cut-off frequency, $f = 2500\ Hz$,

$$|H|\big|_{f=2500\ Hz} = \frac{\sqrt{R^2 + {X_{C_2}}^2}}{\sqrt{R^2 + \left(2\pi(2500 - 3000)L + \frac{3000}{2500}X - X_{C_2}\right)^2}}$$

$$|H|\big|_{f=2500\ Hz} = \frac{\sqrt{R^2 + {X_{C_2}}^2}}{\sqrt{R^2 + \left(-1000\pi L + \frac{6}{5}\frac{1}{6000\pi C_2} - \frac{1}{5000\pi C_1}\right)^2}}$$

Simplify equation above to become Equation (4.23)

$$|H|\big|_{f=2500\ Hz} = \frac{\sqrt{R^2 + {X_{C_2}}^2}}{\sqrt{R^2 + (1000\pi L)^2}} \tag{4.23}$$

Similarly, it is same for upper cut-off frequency, $f = 3500\ Hz$,

$$|H|\big|_{f=3500\ Hz} = \frac{\sqrt{R^2 + {X_{C_2}}^2}}{\sqrt{R^2 + \left(2\pi(3500 - 3000)L + \frac{3000}{3500}X - X_{C_2}\right)^2}}$$

Then expand the $X$and X_{C_2}, as illustrated in Equation

$$|H|\big|_{f=3500\,Hz} = \frac{\sqrt{R^2 + {X_{C_2}}^2}}{\sqrt{R^2 + \left(1000\pi L + \frac{3000}{3500}\frac{1}{6000\pi C_2} - \frac{1}{7000\pi C_1}\right)^2}}$$

The solution is illustrated in Equation (4.24)

$$|H|\big|_{f=3500\,Hz} = \frac{\sqrt{R^2 + {X_{C_2}}^2}}{\sqrt{R^2 + (1000\pi L)^2}} \tag{4.24}$$

Notice that Equation (4.23) equals to Equation (4.24). Therefore

$$|H|\big|_{f=2500\,Hz} = |H|\big|_{f=3500\,Hz} = \frac{1}{\sqrt{2}}|H|_{max} \tag{4.25}$$

where $\frac{1}{\sqrt{2}}$ represents half-power or – 3dB power reduction. Next, substitute the parameters into Equation (4.25) to become Equation (4.26).

$$\frac{\sqrt{R^2 + {X_{C_2}}^2}}{\sqrt{R^2 + (1000\pi L)^2}} = \frac{1}{\sqrt{2}}\frac{\sqrt{R^2 + {X_{C_2}}^2}}{R} \tag{4.26}$$

Simplify Equation (4.26)to obtain the following

$$\sqrt{2}R = \sqrt{R^2 + (1000\pi L)^2}$$

Finally, further simplify the equation above to achieve

$$R = 1000\pi L \tag{4.27}$$

4.3.3 MATHEMATICAL DERIVATION TO FORM RELATIONSHIP BETWEEN C AND L

From the Equation (4.27), the relationship between R and L is derived. So the next step is to derive the equations to express the relationship between L and C_1 and C_2. To simplify the overall calculation, let $C_1 = C_2 = C$. Thus from Equation (4.8), X_L and X are expanded as demonstrated in Equation (4.28).

$$C_1 = \frac{1}{2\pi f_0 (X_L - X)} = \frac{1}{2\pi f_0 \left(2\pi f L - \frac{1}{6000\pi C_2}\right)} \tag{4.28}$$

After that, substitute $f_0 = 3000\ Hz$ into Equation (4.28)

$$C_1 = \frac{1}{6000\pi \left(2\pi f L - \frac{1}{6000\pi C_2}\right)}$$

Rearrange the equation above to become

$$6000\pi C_1 \left(2\pi f L - \frac{1}{6000\pi C_2}\right) = 1$$

Therefore simplify the equation above to form

$$C = \frac{2}{(6000\pi)^2 f L} \tag{4.29}$$

4.3.4 EFFECT OF R AND C ON THE FILTER RESPONSE

Another important factor in designing the adaptive impedance matching circuit is to have a short transient response, while the overshoot and ringing effect are kept at minimum.

The transfer function of the LCRC impedance matching circuit in the form of Laplace transform is

$$H(s) = \frac{R + \frac{1}{sC_2}}{sL + R + \frac{1}{sC_1} + \frac{1}{sC_2}} \tag{4.30}$$

However, the equation above only shows one type of design that is strictly to band-pass filter only. In other words, not only bandwidth specification has been fixed, but also overshoot and ringing effect remains the same. As a result, it is necessary to carry out an investigation on the effect of R and C_2 of the transfer function of the system, which widens the filter specification and allows alteration in terms of filter types, that is from band-pass to low-pass and vice versa.

Firstly, effect of R on the transfer function is examined. From Equation (4.27), suppose that

$$R = k_1(1000\pi L) \tag{4.31}$$

If $k_1 = 1$, then $R = 1000\pi L$. In terms of transfer function, R is directly proportional to the bandwidth. In other words, R increase by two fold, which causes the bandwidth to also increases by two fold. For transient response, R is directly proportional to the damping ratio, ζ. Therefore the higher value of R will yield higher overshoot. Then the lower value of Rwill yield more ringing frequency.

Next, the effect of C_2 on the transfer function is researched. Referring to Equation (4.32)

$$C_2 = \frac{1}{6000\pi X} \tag{4.32}$$

where X is

$$X = 2\pi fL - \frac{1}{2\pi f C_1} \tag{4.33}$$

As $f = 3000\ Hz$, and let $k_2 = \frac{C_2}{C_1}$, it follows that Equation (4.32)can be rearranged to become

$$C_2 = \frac{1 + k_2}{(6000\pi)^2 L} \tag{4.34}$$

It is known that from Equation (4.29), if$C_1 = C_2$, then

$$C_2 = \frac{2}{(6000\pi)^2 L}$$

Thus, it implies that k_2= 1 if $C_1 = C_2$by equating Equation (4.29) and Equation (4.34).

According to final value theorem,

$$\lim_{t\to\infty} h(t) = \lim_{s\to 0} sH(s)$$

Hence, if $k_2 \to 0$, the filter behaves as low pass filter. But if $k_2 \to \infty$, the filter become the band-pass filter. Besides, by finding its transient response, it will be proven that k_2 play an important role in determining the steady-state value as demonstrated below.

Now, let the sum of the reciprocal of C_1 and C_2 become the sum of the reciprocal of C. Thus,

$$\frac{1}{C_1}+\frac{1}{C_2}=\frac{1}{C}$$

Since $C_1 = C_2$, then $k_2 = 1$

$$\frac{1}{C}=\frac{1}{C_2}+\frac{1}{C_2}=\frac{2}{C_2}$$

$$\frac{1}{C}=\frac{2}{\frac{2}{(6000\pi)^2 L}}=(6000\pi)^2 L$$

If $C_1 = \frac{C_2}{100}$, then $k_2 = 100$. Subsequently,

$$\frac{1}{\frac{C_2}{100}}+\frac{1}{C_2}=\frac{1}{C}$$

And then

$$\frac{1}{C}=\frac{101}{C_2}=\frac{101}{\frac{101}{(6000\pi)^2 L}}=(6000\pi)^2 L$$

So it is confirmed that

$$\frac{1}{C}=(6000\pi)^2 L \qquad (4.35)$$

regardless of k_2.

By rearranging the transfer function,

$$H(s) = \frac{s\left(\frac{R}{L}\right) + \frac{1}{LC_2}}{s^2 + \frac{R}{L}s + \frac{1}{LC}} = \frac{2\zeta\omega_n s + {\omega_d}^2}{s^2 + 2\zeta\omega_n s + {\omega_n}^2} \tag{4.36}$$

Thus by comparing the left hand side and right hand side of the equation,

$${\omega_n}^2 = \frac{1}{LC} \tag{4.37}$$

$$2\zeta\omega_n = \frac{R}{L} \tag{4.38}$$

$${\omega_d}^2 = \frac{(6000\pi)^2}{1 + k_2} \tag{4.39}$$

Substitute Equation (4.35)into Equation (4.37) to become the following equation

$${\omega_n}^2 = (6000\pi)^2 \tag{4.40}$$

Thus

$$\omega_n = 6000\pi \tag{4.41}$$

Then, substitute Equation (4.41) into Equation (4.34)

$$2\zeta(6000\pi) = \frac{R}{L} \tag{4.42}$$

Next, substitute Equation (4.27) into Equation (4.38) to form

$$\zeta = \frac{k_1(1000\pi L)}{2(6000\pi)L} = \frac{k_1}{12} \tag{4.43}$$

For underdamped case, $\zeta < 1$. Consequently, $k_1 < 12$. Meanwhile for critically-damped case, $\zeta = 1$, and thus $k_1 = 12$.

It is known that

$$H(s) = \frac{Y(s)}{X(s)} \Leftrightarrow Y(s) = H(s)X(s)$$

For step response,

$$X(s) = \frac{1}{s}$$

$$Y(s) = \frac{2\alpha s + {w_d}^2}{s(s^2 + 2\zeta\omega_n s + {\omega_n}^2)}$$

In order to find factors of $s^2 + 2\zeta\omega_n s + {\omega_n}^2$

$$s = \frac{-(2\zeta\omega_n) \pm \sqrt{(2\zeta\omega_n)^2 - 4(1)({\omega_n}^2)}}{2(1)}$$

Note that it is desirable to obtain system with underdamped case (that is $\zeta < 1$). Therefore,

$$s = -\zeta\omega_n \pm \omega_n\sqrt{\zeta^2 - 1} = -\alpha \pm j\beta$$

where

$$\alpha = \zeta\omega_n$$

$$\beta = \omega_n\sqrt{1-\zeta^2}$$

As a result, $s^2 + 2\zeta\omega_n s + {\omega_n}^2 = (s+\alpha+j\beta)(s+\alpha-j\beta)$with $\zeta < 1$.Next, perform partial fraction on $Y(s)$.

$$Y(s) = \frac{2\alpha s + {w_d}^2}{s(s+\alpha+j\beta)(s+\alpha-j\beta)} = \frac{A}{s} + \frac{B}{s+\alpha+j\beta} + \frac{C}{s+\alpha-j\beta} \tag{4.44}$$

It is known that from Heaviside cover-up method, it is determined as follows;

$$A = \frac{{w_d}^2}{\alpha^2+\beta^2} \tag{4.45}$$

$$B = \frac{-2\alpha(-\alpha-j\beta) + {w_d}^2}{(-\alpha-j\beta)(2j\beta)} \tag{4.46}$$

$$C = \frac{-2\alpha(-\alpha+j\beta) + {w_d}^2}{(-\alpha+j\beta)(2j\beta)} = B^* \tag{4.47}$$

Since

$$\alpha^2+\beta^2 = (\zeta\omega_n)^2 + \left(\omega_n\sqrt{\zeta^2-1}\right)^2 = {\omega_n}^2$$

Thus substitute Equation (4.40) into Equation (4.45), and it yields;

$$A = \frac{{w_d}^2}{\alpha^2+\beta^2} = \frac{\frac{{\omega_n}^2}{1+k_2}}{{\omega_n}^2} = \frac{1}{1+k_2} \tag{4.48}$$

Rearrange Equation (4.46) and Equation (4.47) to become

$$B = -\frac{j(2\alpha^2 - 2j\alpha\beta - {w_d}^2)}{2(\alpha - j\beta)(\beta)} \tag{4.49}$$

$$C = \frac{j(2\alpha^2 + 2j\alpha\beta - {w_d}^2)}{2(\alpha + j\beta)(\beta)} \tag{4.50}$$

Thus, Equation (4.40) can be simplified as

$$Y(s) = \frac{\frac{1}{1+k_2}}{s} + \frac{-\frac{j(2\alpha^2 - 2j\alpha\beta - {w_d}^2)}{2(\alpha - j\beta)(\beta)}}{s + \alpha + j\beta} + \frac{\frac{j(2\alpha^2 + 2j\alpha\beta - {w_d}^2)}{2(\alpha + j\beta)(\beta)}}{s + \alpha - j\beta}$$

$$Y(s) = \frac{\frac{1}{1+k_2}}{s} + \frac{-\frac{2\alpha^3 + 2\alpha\beta^2 + s{w_d}^2}{\alpha^2 + \beta^2}}{s^2 + 2\alpha s + (\alpha^2 + \beta^2)} \tag{4.51}$$

Then, perform inverse Laplace transform on Y(s) in order to obtain step-response y(t)

It is known that

$$\begin{cases} \mathcal{L}^{-1}\left\{\frac{1}{s}\right\}(t) = u(t), \\ \mathcal{L}^{-1}\left\{\frac{1}{s^2+2\alpha s+\alpha^2+\beta^2}\right\}(t) = \mathcal{L}^{-1}\left\{\frac{1}{(s+\alpha)^2+\beta^2}\right\} = \frac{1}{\beta}e^{-\alpha t}sin\beta t, \text{and} \\ \mathcal{L}^{-1}\left\{\frac{s+\alpha}{s^2+2\alpha s+\alpha^2+\beta^2}\right\}(t) = \mathcal{L}^{-1}\left\{\frac{s+\alpha}{(s+\alpha)^2+\beta^2}\right\} = e^{-\alpha t}cos\beta t \end{cases}$$

Thus,

$$\mathcal{L}^{-1}\left\{\frac{-\frac{2\alpha^3 + 2\alpha\beta^2 + s{w_d}^2}{\alpha^2 + \beta^2}}{s^2 + 2\alpha s + (\alpha^2 + \beta^2)}\right\}(t) = \mathcal{L}^{-1}\left\{\frac{-\frac{2\alpha^3 + 2\alpha\beta^2 - \alpha{w_d}^2}{\alpha^2 + \beta^2} - \frac{s{w_d}^2 + \alpha{w_d}^2}{\alpha^2 + \beta^2}}{s^2 + 2\alpha s + (\alpha^2 + \beta^2)}\right\}(t)$$

Since

$$\mathcal{L}^{-1}\left\{\frac{-\frac{2\alpha^3+2\alpha\beta^2-\alpha{w_d}^2}{\alpha^2+\beta^2}}{s^2+2\alpha s+(\alpha^2+\beta^2)}\right\}(t)=-\frac{2\alpha^3+2\alpha\beta^2-\alpha{w_d}^2}{\beta(\alpha^2+\beta^2)}e^{-\alpha t}sin\beta t$$

And

$$\mathcal{L}^{-1}\left\{\frac{-\frac{s{w_d}^2+\alpha{w_d}^2}{\alpha^2+\beta^2}}{s^2+2\alpha s+(\alpha^2+\beta^2)}\right\}(t)=\frac{{w_d}^2}{\alpha^2+\beta^2}e^{-\alpha t}cos\beta t$$

Therefore,

$$y(t)=\frac{1}{1+k_2}u(t)+-\frac{2\alpha^3+2\alpha\beta^2-\alpha{w_d}^2}{\beta(\alpha^2+\beta^2)}e^{-\alpha t}sin\beta t+\frac{{w_d}^2}{\alpha^2+\beta^2}e^{-\alpha t}cos\beta t \quad (4.52)$$

is the step response of impedance matching filter.

Therefore, steady-state value y(∞) = $\frac{1}{1+k_2}$. It can be seen that if if $k_2 \to 0$, y(∞) = 1 while if $k_2 \to \infty$, y(∞) = 0.

4.3.5 DERIVATION OF LOAD IMPEDANCE RELATED TO INPUT PARAMETERS

In order to determine load impedanceZ_p, it is required to fulfil maximum power transfer. Thus, it is desired to achieve half of the input voltage at the output, that is

$$v_{out}(t)=\frac{1}{2}v_{in}(t) \quad (4.53)$$

According to voltage divider rule,

$$v_{out}(t) = \frac{Z_x}{Z_x + j\left(X_L - X_{C_1}\right) + Z_s} v_{in}(t) \tag{4.54}$$

where$Z_x = (R - jX_{C_2}) \,||\, Z_p$, $Z_p = (R_p + jX_p)$,$X_p > 0$ and $Z_s = (R_s + jX_s)$. In addition to that, $X_{C_1}, X_{C_2}$and X_L are related by following equations

$$\begin{cases} X_{C_1} = \dfrac{1}{2\pi f C_1}, \\ X_{C_2} = \dfrac{1}{2\pi f C_2} \\ X_L = 2\pi f L \end{cases} \tag{4.55}$$

Substituting Equation (4.53) into Equation (4.54), it yields

$$j\left(X_L - X_{C_1}\right) + Z_s = Z_x$$

$$j\left(X_L - X_{C_1}\right) + (R_s + jX_s) = \frac{(R - jX_{C_2})(R_p + jX_p)}{\left(R - jX_{C_2}\right) + \ (R_p + jX_p)}$$

$$R_s + j\left(X_s + X_L - X_{C_1}\right) = \frac{(R - jX_{C_2})(R_p + jX_p)}{(R + R_p) + j(X_p - X_{C_2})}$$

$$R_s + j\left(X_s + X_L - X_{C_1}\right) = \frac{\left(RR_p + X_{C_2}X_p\right) + j(RX_p - R_pX_{C_2})}{(R + R_p) + j(X_p - X_{C_2})}$$

$$R_s + j\left(X_s + X_L - X_{C_1}\right) = \frac{\left(RR_p + X_{C_2}X_p\right) + j(RX_p - R_pX_{C_2})}{\left(R + R_p\right) + j(X_p - X_{C_2})} \tag{4.56}$$

By equating real and imaginary parts of both sides of Equation (4.56), it yields

$$\begin{cases} R_s(R + R_p) - (X_p - X_{C_2})(X_s + X_L - X_{C_1}) = RR_p + X_{C_2}X_p & (4.57) \\ R_s(X_p - X_{C_2}) + \left(R + R_p\right)\left(X_s + X_L - X_{C_1}\right) = RX_p - R_pX_{C_2} & (4.58) \end{cases}$$

From Equation (4.57), it can be rearranged to

$$X_p(X_s + X_L + X_{C_2} - X_{C_1}) = R_sR + R_sR_p - RR_p + X_{C_2}(X_s + X_L - X_{C_1})$$

$$X_p = \frac{R_p(R_s - R) + R_s R + X_{C_2}(X_s + X_L - X_{C_1})}{\left(X_s + X_L + X_{C_2} - X_{C_1}\right)} \tag{4.59}$$

From Equation (4.58), it can be rearranged to

$$R_p(X_s + X_L + X_{C_2} - X_{C_1}) = RX_p - R_s(X_p - X_{C_2}) - R(X_s + X_L - X_{C_1})$$

$$R_p = \frac{X_p(R - R_s) + R_s X_{C_2} - R(X_s + X_L - X_{C_1})}{\left(X_s + X_L + X_{C_2} - X_{C_1}\right)} \tag{4.60}$$

Substituting Equation (4.59) into Equation (4.60), it yields

$$R_p = \frac{\left(\frac{R_p(R_s - R) + R_s R + X_{C_2}\left(X_s + X_L - X_{C_1}\right)}{\left(X_s + X_L + X_{C_2} - X_{C_1}\right)}\right)(R - R_s) + R_s X_{C_2} - R(X_s + X_L - X_{C_1})}{\left(X_s + X_L + X_{C_2} - X_{C_1}\right)}$$

Let $k_3 = X_s + X_L + X_{C_2} - X_{C_1}$

$$R_p = \left(\frac{R_p(R_s - R) + R_s R + X_{C_2}\left(X_s + X_L - X_{C_1}\right)}{{k_3}^2}\right)(R - R_s) + \frac{R_s X_{C_2}}{k_3} - R\frac{X_s + X_L - X_{C_1}}{k_3}$$

$$R_p\left(1 + \frac{(R_s - R)^2}{{k_3}^2}\right) = \left(\frac{R_s R + X_{C_2}\left(X_s + X_L - X_{C_1}\right)}{{k_3}^2}\right)(R - R_s) + \frac{R_s X_{C_2}}{k_3} - R\frac{X_s + X_L - X_{C_1}}{k_3}$$

$$R_p = \frac{\left(\frac{R_s R + X_{C_2}\left(X_s + X_L - X_{C_1}\right)}{{k_3}^2}\right)(R - R_s) + \frac{R_s X_{C_2}}{k_3} - R\frac{X_s + X_L - X_{C_1}}{k_3}}{1 + \frac{(R_s - R)^2}{{k_3}^2}} \tag{4.61}$$

in which R_p is expressed in term of all relevant input parameters. Similarly, X_p can be expressed as

$$X_p = \frac{\left(\frac{R_s X_{C_2} - R\left(X_s + X_L - X_{C_1}\right)}{{k_3}^2}\right)(R_s - R) + \frac{R_s R}{k_3} + X_{C_2}\frac{X_s + X_L - X_{C_1}}{k_3}}{1 + \frac{(R_s - R)^2}{{k_3}^2}} \tag{4.62}$$

4.3.6 PROPOSED ALGORITHM OF IMPEDANCE MATCHING

L is the key parameter of the filter to determine the R, C_1 and C_2, which is illustrated in Equation (4.31) and Equation (4.34). At the same time, relationship of $Z_p, Z_s,$ L, R, C_1 and C_2 are summarised in Equation (4.55), Equation (4.61) and Equation (4.62). As a result, it follows that L can be determined by exploiting Equation (4.55), Equation (4.61) and Equation (4.62)given Z_p and Z_s and filter design derived from Equation (4.31) and Equation (4.34). It is discovered that it becomes a cubic equation in term of L, which is in form of $aL^3 + bL^2 + c\mathrm{L} + \mathrm{d} = 0$, upon substitution, rearrangement and term collection. Therefore, the problem of feasibility study on impedance matching is reducible to problem of solving cubic equation. The finding of value of L can be simplified according to the following algorithm.

1. Initialize expression $aL^3 + bL^2 + c\mathrm{L} + \mathrm{d}$
2. Initialize Z_p , Z_s to determine coefficients of b, c and d
3. Establish k_1, $k_2$and f to determine coefficients of a, b and c
4. Solve cubic equation $aL^3 + bL^2 + c\mathrm{L} + \mathrm{d} = 0$
5. If solutions of step 4 meet the condition of $L \in \mathbb{R}$ and L > 0, then it is completed. Otherwise, re-establish k_1 and k_2 and solve again by repeating step 3 and 4.

It is known that from fundamental theorem of algebra, that if the degree of a real polynomial is odd, it must have at least one real root. In this case, the degree of cubic equation $aL^3 + bL^2 + c\mathrm{L} +$ dis 3, which is odd. Therefore, at least one of the solution of L must be real. It implies that the solutions of L are either three real roots or a real root

and complex conjugate pair roots. It is interesting to observe that Step 4 of the algorithm above always produce one negative real root, which is unacceptable. It means that it is left with other solutions, which can be either two real roots or complex conjugate pair roots. If complex conjugate pair roots occur, then filter specification can be loosened by increasing eitherk_1 or$k_2$without changing f, Z_p and Z_s.

Suppose that k_1= 1, $k_2 = 100$ and f = 3000, by considering Equation (4.61), it yields relationship relating R_p , R_s , X_s and L as shown in the following

$$aL^3 + bL^2 + c\mathrm{L} + \mathrm{d} = 0 \tag{4.63}$$

$$\text{with} \begin{cases} a = 1.094 \times 10^8 \\ b = 1.094 \times 10^8 R_p - 9.904 \times 10^6 R_s + 1.173 \times 10^6 X_s \\ c = \left(\frac{24000\pi X_s}{101} - 2000\pi R_s\right) R_p + (1000\pi)\left({R_s}^2 + {X_s}^2\right) \\ d = R_p({R_s}^2 + {X_s}^2) \end{cases}$$

Given that $R_p = 16\ \Omega$, , $R_s = 11\ \Omega$ and $X_s = 0.2\ \Omega$, then L can be determined from Equation (4.63), which are 14.9mH, -282 mH and 3.60 mH. Thus, the suitable solutions of L are 14.9 mH and 3.60 mH, which lead to two distinct X_p according to Equation (4.62). By inspection, L = 14.9 mH yields $X_p = 5.27\ \Omega$ while L = 3.6 mH yields $X_p = 78.14\ \Omega$. However, suitable X_p can be found by using Equation (4.59)and $R_p = 16\ \Omega$, which yields $X_p = 5.27\ \Omega$. In short, $[R_p, X_p] = [16, 5.27]\ \Omega$ leads to L = 14.9 mH, which can be further confirmed in the next subchapter.

4.4 EXPERIMENT

This subchapter describes the methods used to validate the concept. Similar to Chapter 3, the concept can be validated through theoretical analysis and practical analysis. The theoretical analysis used in this subchapter consists of software simulations, which are

simulated using both PSIM and MATLAB. For the meantime, the practical analysis used in this subchapter is the experimental analysis using the electronic components in the laboratory.

4.4.1 SIMULATION RESULT

Figure 4.1 aforementioned illustrated the circuit diagram of the LCRC impedance matching circuit, which is drawn using PSIM. In this simulation, the input voltage, V_{in} is 10 V peak, and the central frequency, f_0 is 3 kHz. In the actual application of narrowband power line communication, the modulated signal is generated from the computer or laptop to the electrical appliances. Thus the source impedance, Z_s of the laptop can be assumed as $11 + j0.2\ \Omega$.

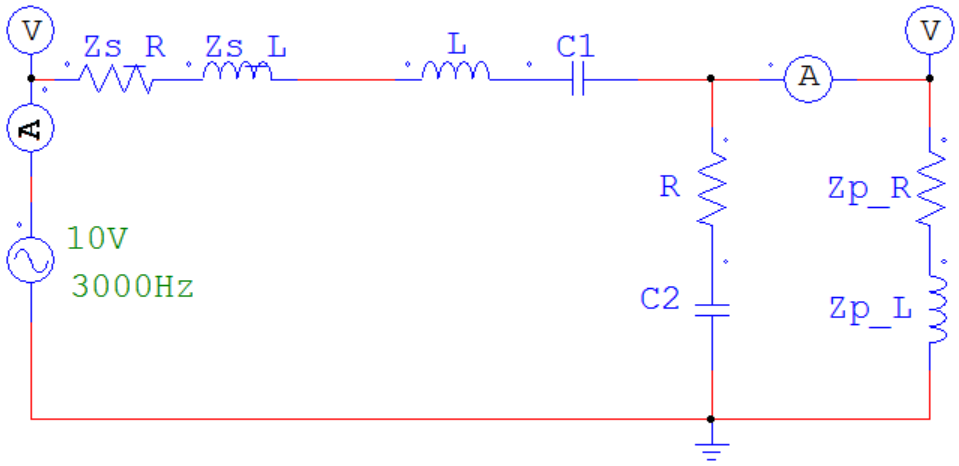

Figure 4.5: PSIM drawing of PLC with the LCRC impedance matching circuit

Table 4.1shows the types of loads used and its impedance value in the experiment. Notice that Load 1 and 2 has the same resistance but they have different polarity of reactance. The same situation applies to Load 3 and 4. The purpose of the selective loads used in this experiment is to test the feasibility of the impedance matching circuit when it encounters different types of load, in which it is either inductive or capacitive reactance load.

	Load Impedance, Z_p	
Load type	**Resistance (Ω)**	**Reactance (Ω)**
Load 1	16	5.27
Load 2	16	−5.27
Load 3	14	5.28
Load 4	14	−5.28

Table 4.1: Types of loads used and its impedance value

In the meantime, Table 4.2 tabulates the inductance, resistance and capacitance value of the circuit, in which they can be calculated using the Equation.

Load type	**Inductance, L (mH)**	**Capacitance, C1 (µF)**	**Resistance, R (Ω)**	**Capacitance, C2(µF)**
Load 1 & 2	10	0.284	31	28
Load 3 & 4	15	0.189	47	18

Table 4.2: Calculated inductance, resistance and capacitances value

Figure 4.6, Figure 4.8, Figure 4.10 and Figure 4.12 illustrates the PSIM drawing of LCRC impedance matching circuit with Load 1, Load 2, Load 3 and Load 4 respectively. Meanwhile, Figure 4.7, Figure 4.9, Figure 4.11, Figure 4.13 display the PSIM simulation for voltage and current waveform for Load 1, Load 2, Load 3 and Load 4 respectively. Based on all the simulation results, it is clearly shown that with various types of load impedance applied to the circuit, the output voltage, V_{out} is half of the input voltage, V_{in}. Hence, it is verified that the LCRC impedance matching circuit has successfully achieve maximum power transfer in this system.

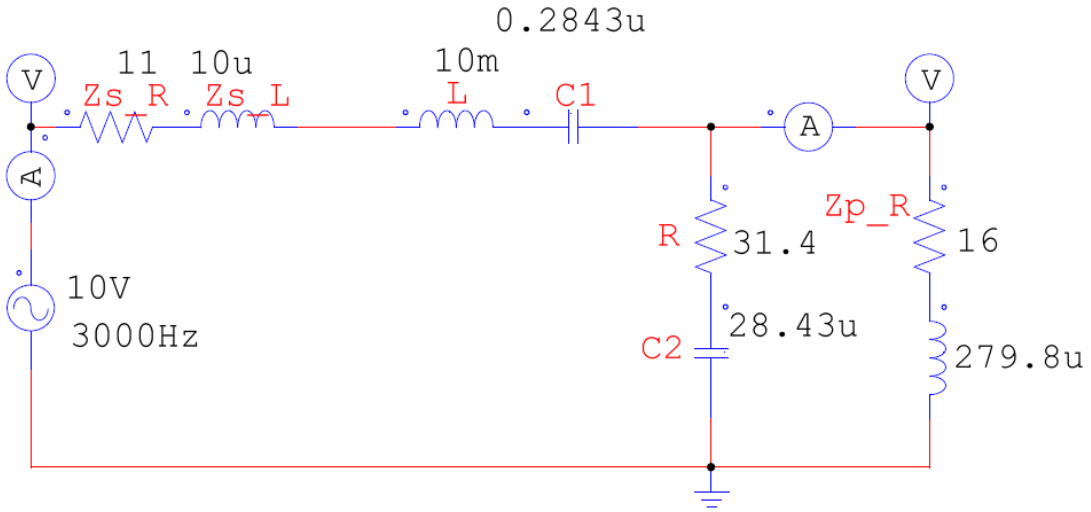

Figure 4.6: PSIM drawing of LCRC impedance matching circuit for Load 1

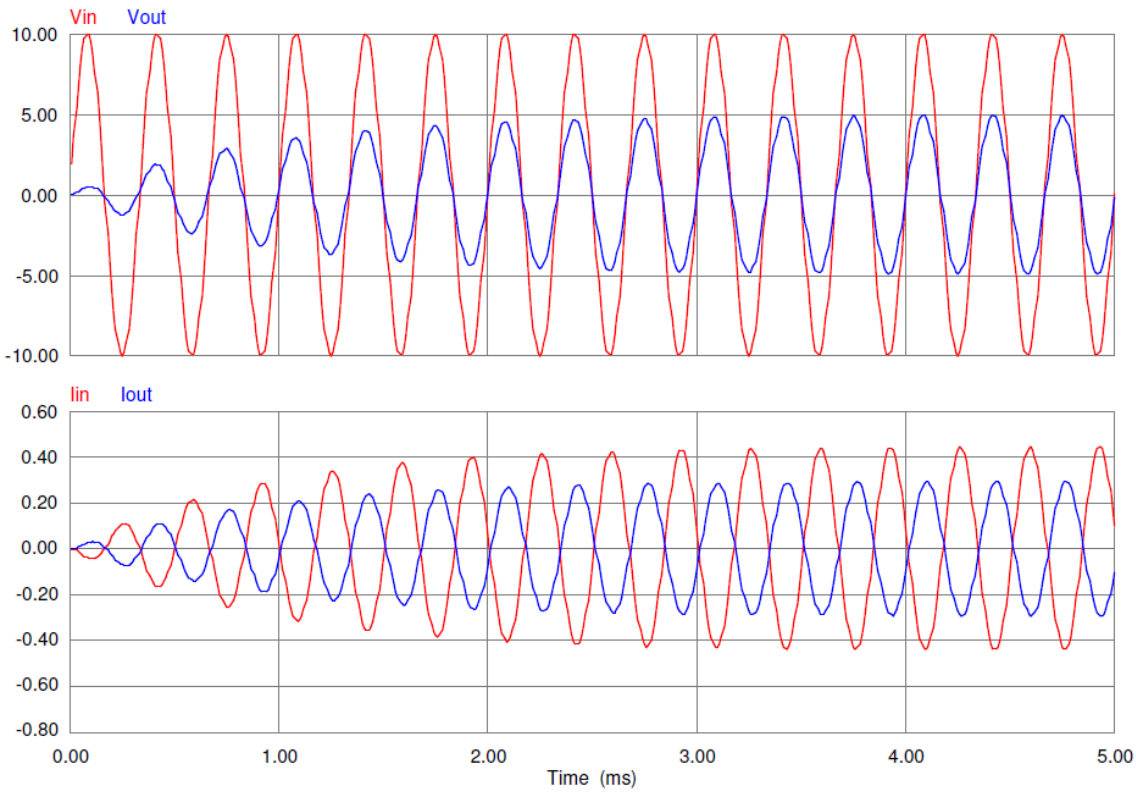

Figure 4.7: PSIM simulation for voltage and current waveform for Load 1

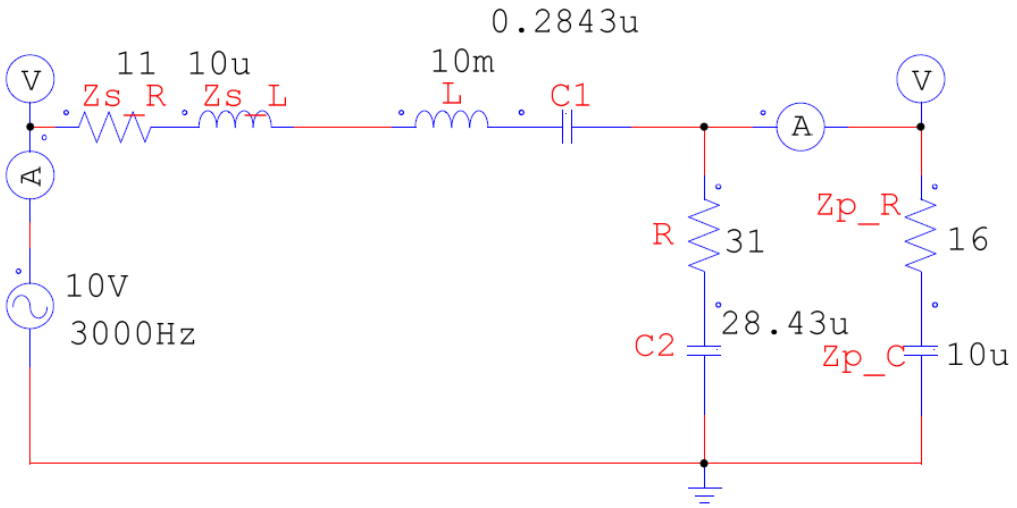

Figure 4.8: PSIM drawing of LCRC impedance matching circuit for Load 2

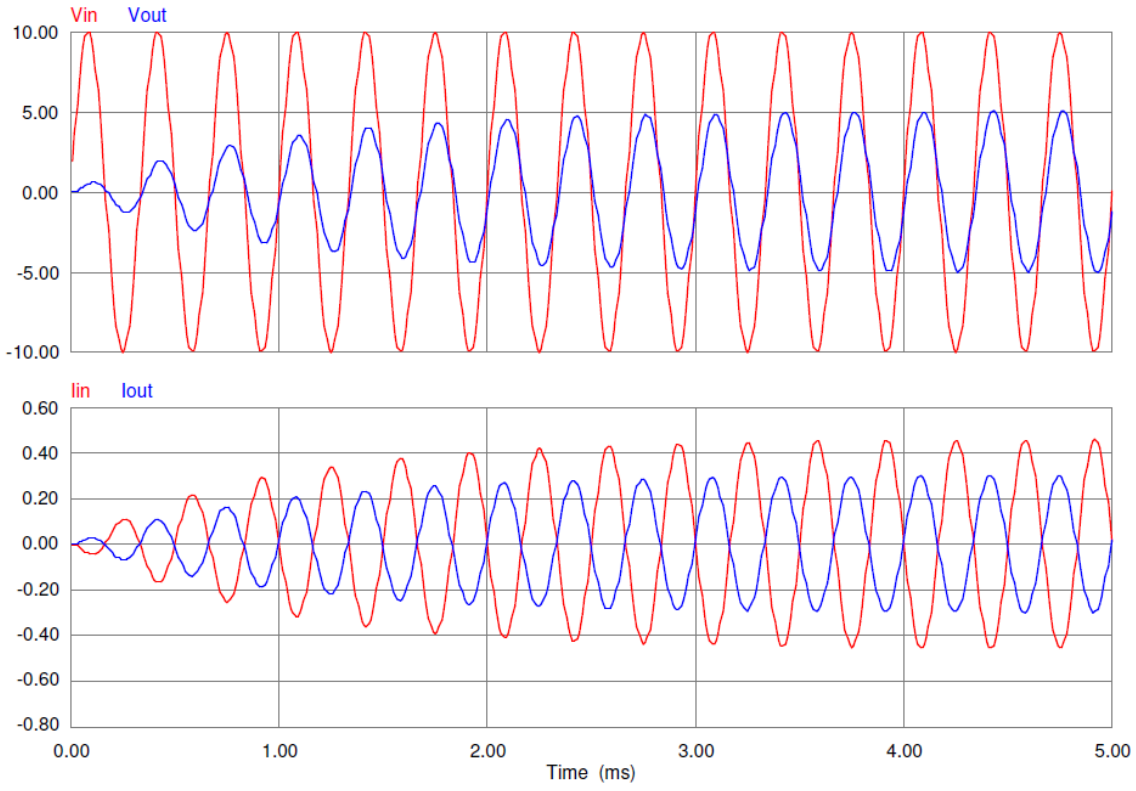

Figure 4.9: PSIM simulation for voltage and current waveform for Load 2

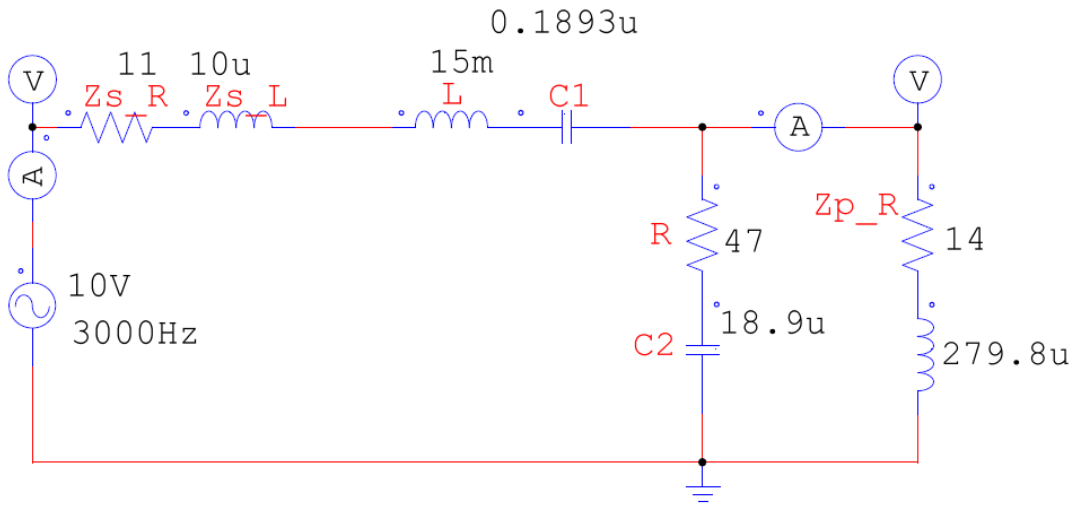

Figure 4.10: PSIM drawing of LCRC impedance matching circuit for Load 3

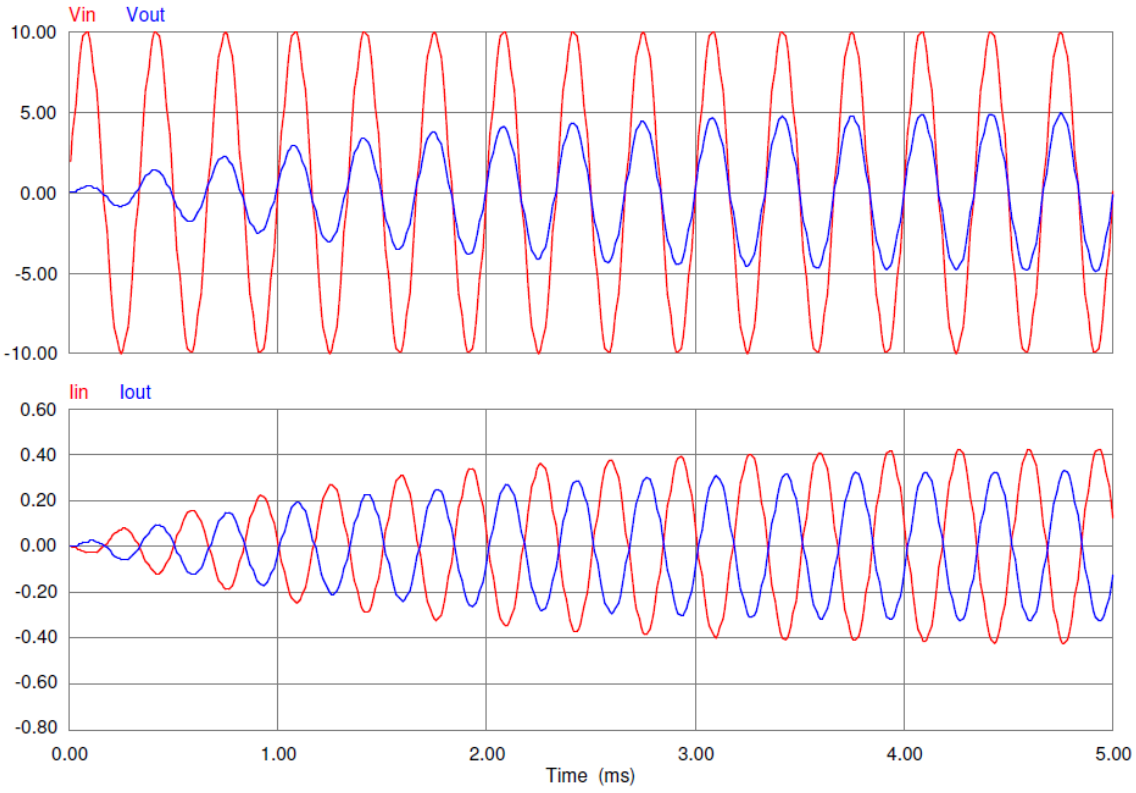

Figure 4.11: PSIM simulation for voltage and current waveform for Load 3

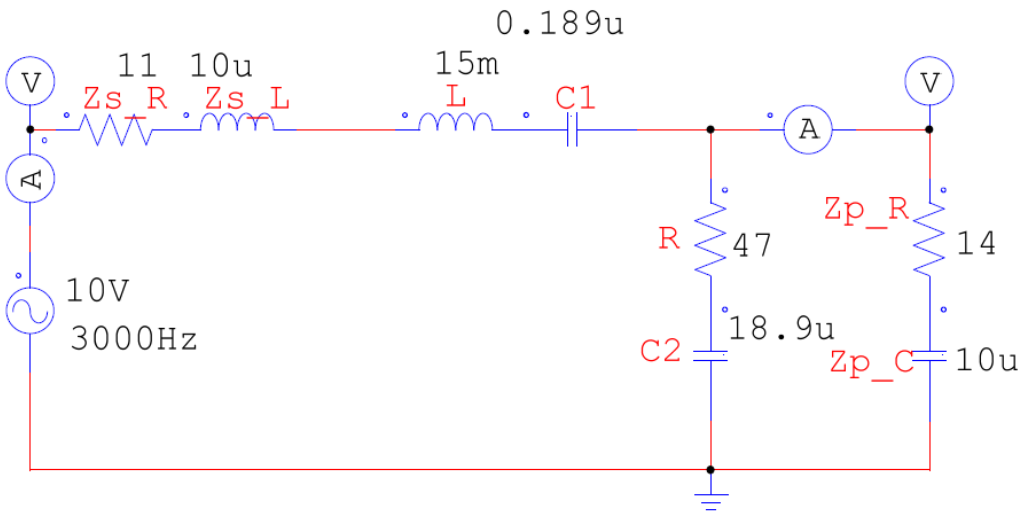

Figure 4.12: PSIM drawing of LCRC impedance matching circuit for Load 4

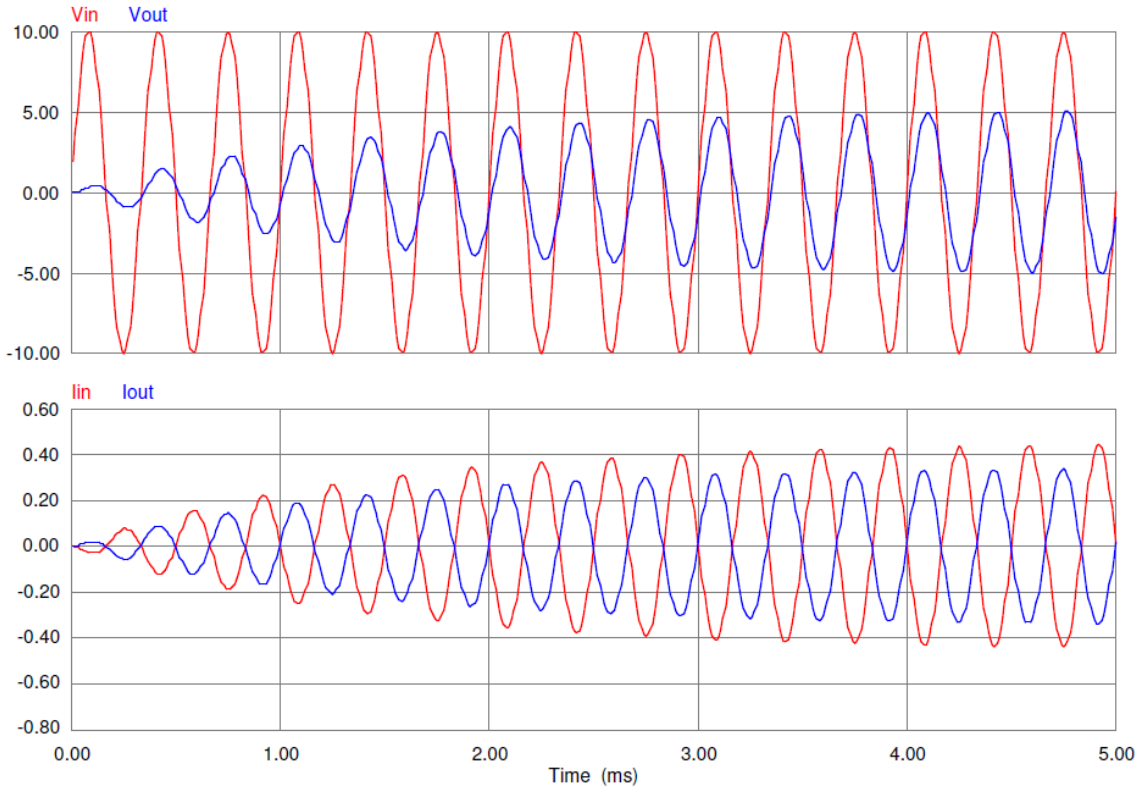

Figure 4.13: PSIM simulation for voltage and current waveform for Load 4

Since LCRC is a newly proposed circuit model, it is essential to investigate whether the modulated frequency signal can pass through the matching circuit. At the same time, it is

also important to study the step response of the matching circuit. After performing various MATLAB simulations, it can be noticed that LCRC can be either a low-pass filter or a band-pass filter, depending on the parameters of the component used in the matching circuit. By using the component parameters given in Table 4.1 and Table 4.2, the MATLAB simulations for magnitude plot and step response has been illustrated in Figure 4.14 and Figure 4.15 respectively for Load 1 and 2 circuits, likewise in Figure 4.16 and Figure 4.17 respectively for Load 3 and 4 circuits.

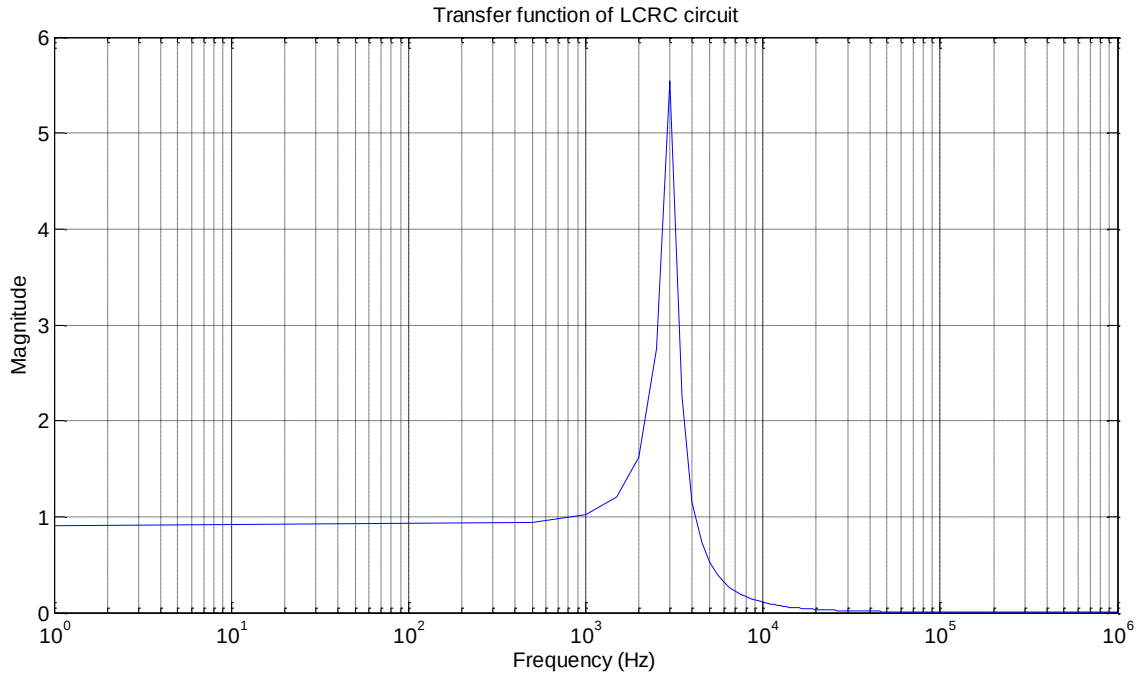

Figure 4.14: MATLAB simulation for magnitude plot of the circuit for Load 1 and 2

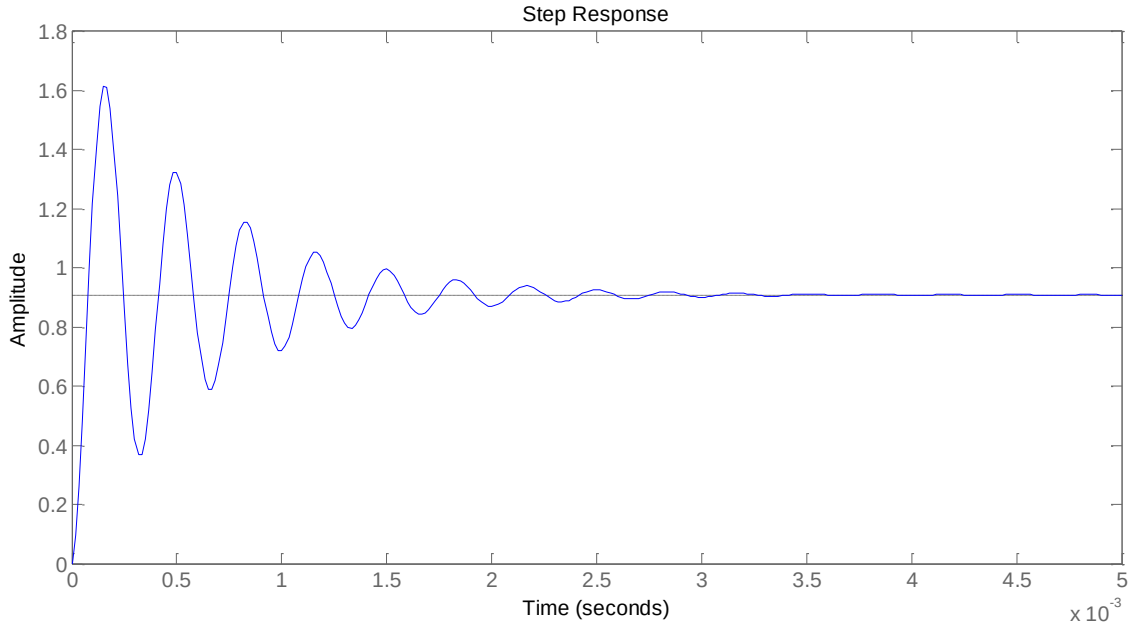

Figure 4.15: MATLAB simulation for step response of the circuit for Load 1 and 2

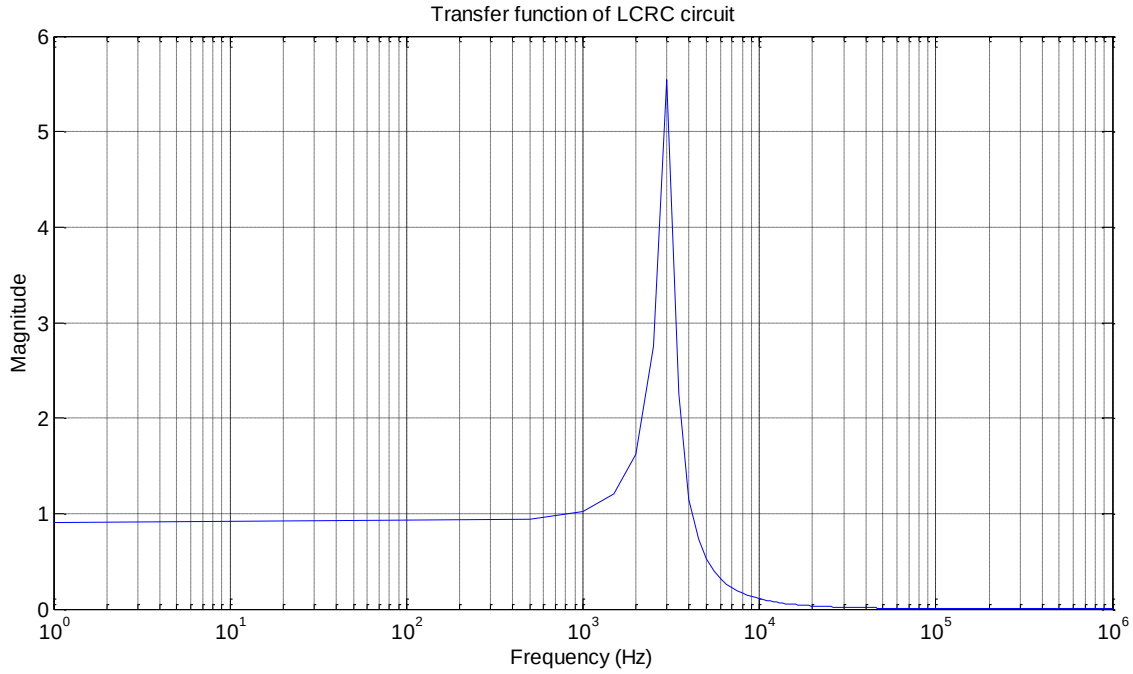

Figure 4.16: MATLAB simulation for magnitude plot of the circuit for Load 3 and 4

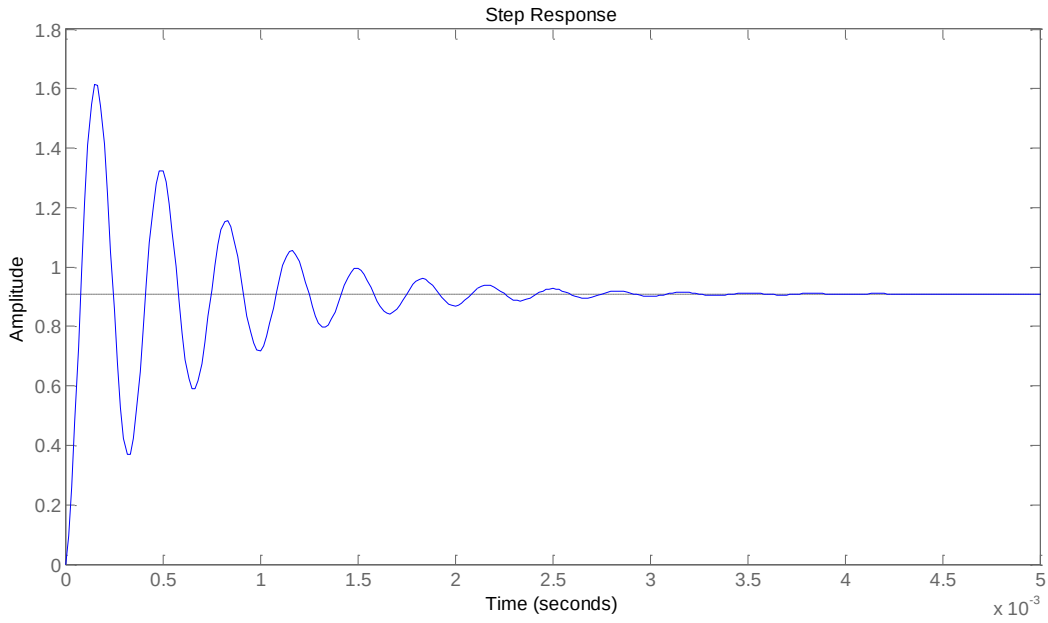

Figure 4.17: MATLAB simulation for step response of the circuit for Load 3 and 4

From the magnitude plot shown in Figure 4.14 and Figure 4.16, it is clearly demonstrated that the LCRC is now a low-pass filter. However, there are several problems that can be observed from the MATLAB simulations. For instance, the low frequency noises are able to pass through the matching circuit. In additional, since the system is underdamped, the maximum overshoot of the step response displayed in Figure 4.15 and Figure 4.17 are slightly high, which are 60% for both cases. Besides, after many trials and errors, this method is limited to the source and channel impedances that have relatively low resistance, less than 40 Ω in order to ensure the modulated frequency can pass through the circuit in ideal manner. Hence it is necessary to have a passive high-pass filter to filter out the low frequency noises, and implement the PID controller proposed in [30] to control the overshoot and the ringing effect of the transient response, and increase the impedance range of the impedance matching.

4.4.2 MEASURED RESULT

After the simulation verification had been completed, the next step is to verify the concept through practical analysis. The circuit diagram shown in Figure 4.5 had been constructed using the electronic components that are available in the laboratory. In the meantime, function generator is the voltage source and also the source of the modulated frequency. Then, an oscilloscope is used to measure the voltage waveform at both input and output voltage of the circuit.

The parameter of this experiment is identical to the parameters set in the PSIM simulations. Hence, the input voltage is remained as 10 V peak, the generated frequency is 3 kHz. After that, the measured result is compared with the theoretical analysis to identify the feasibility of the concept in practical situation. However, due to the limitation of the equipment in the laboratory, there are several problems encountered during the practical experiments. Firstly, the overall impedance of the circuit is relatively small. Therefore, the measured result was deviated initially because of the 50 Ω internal resistance comes from the function generator. Thus, in order to solve this problem, it is necessary to add an additional resistor of 50 Ω in series with both of the R of the matching circuit and the load impedance, Z_s to match the circuit in this experiment. Figure 4.18, Figure 4.19, Figure 4.20 and Figure 4.21 show the voltage waveforms from the oscilloscope for Load 1, Load 2, Load 3 and Load 4 respectively.

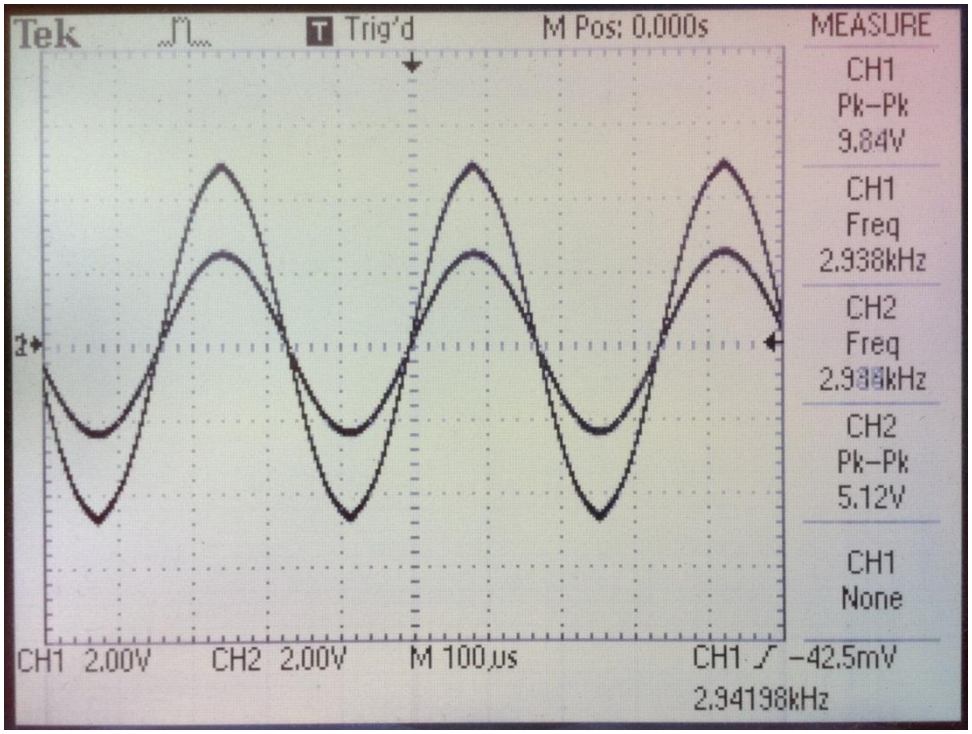

Figure 4.18: Oscilloscope measurement for voltage waveform for Load 1

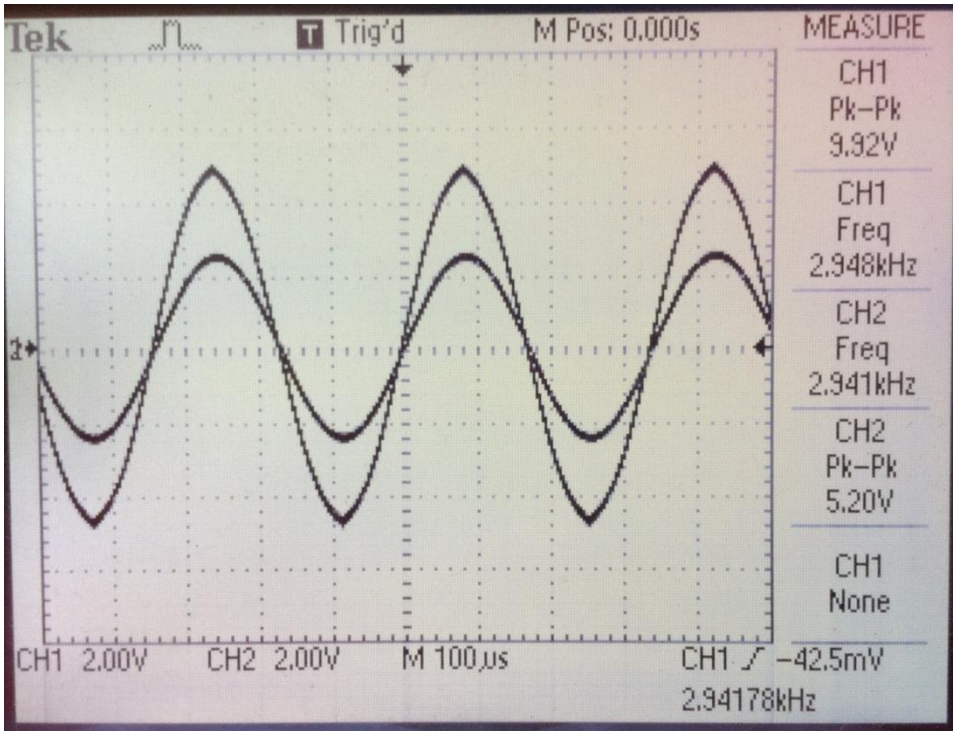

Figure 4.19: Oscilloscope measurement for voltage waveform for Load 2

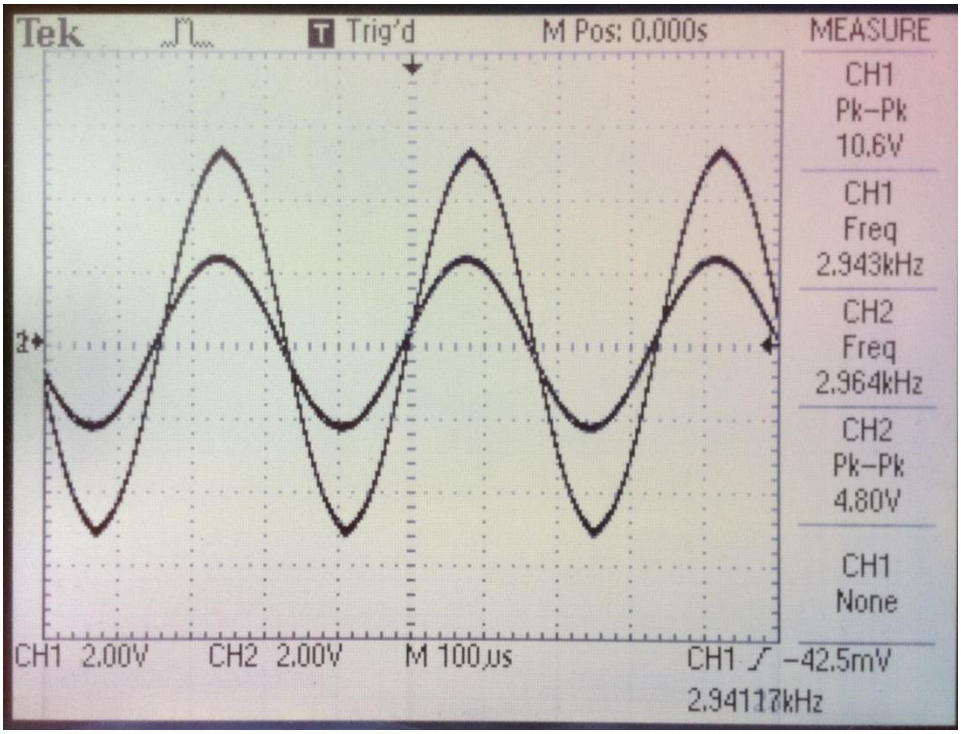

Figure 4.20: Oscilloscope measurement for voltage waveform for Load 3

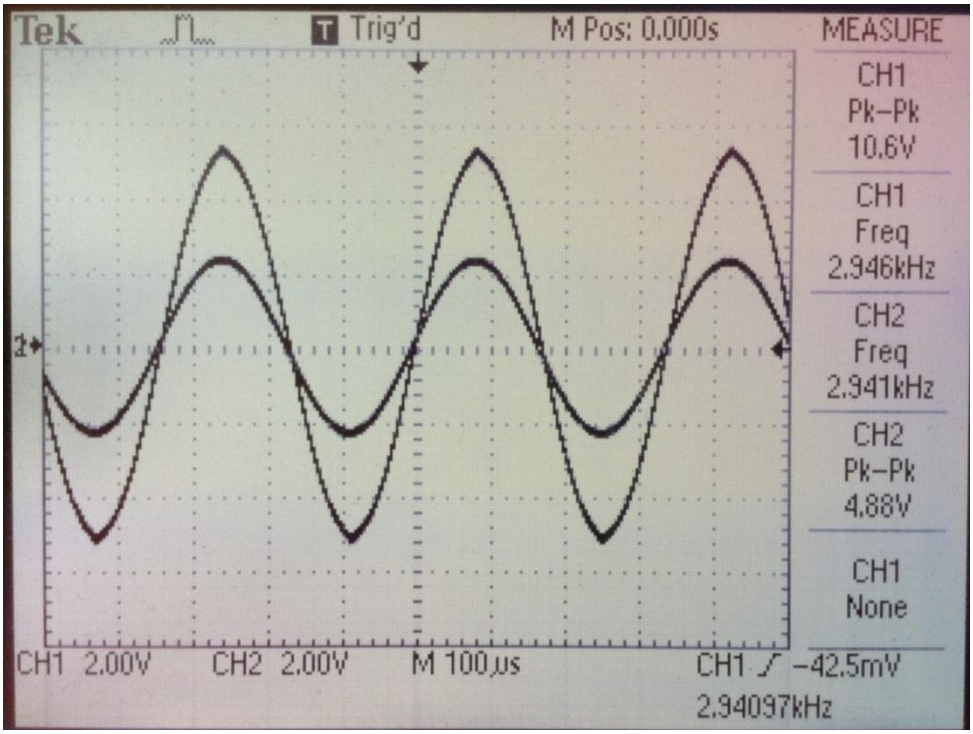

Figure 4.21: Oscilloscope measurement for voltage waveform for Load 4

Based on the measurement results given in Figure 4.18, Figure 4.19, Figure 4.20 and Figure 4.21, it is clearly shown that the output voltage is half of the input voltage. So, the maximum power transfer can be observed from this experiment. But then the practical experiment of step response was unable to be performed due to the internal impedance coming from the function generator, which greatly affects the value of the source impedance.

Still, the concept LCRC impedance matching circuit is practical to be used in the actual application of narrowband power line communication, with the requirement of implementing the passive high-pass filter and PID controller in the system to filter out the noise and control the maximum overshoot of the transient response respectively.

4.5 SUMMARY

This chapter proposed another new methodology of impedance matching for NB-PLC channel. This method has solved the problem stated in Chapter 3, in which it can match the source and channel impedances with inclusive of reactance continuously. Thus, maximum power transfer can be achieved. And of course, this method has advantage in higher matching resolution than the method in Chapter 3. This method has been tested and verified through PSIM and MATLAB simulation, and it has also been tested in the laboratory to ensure it is feasible to use in the actual application of NB-PLC, in order to reduce noise level and impedance mismatch. However, in order to ensure the modulated frequency can pass through the circuit in the ideal manner, this method is limited to the source and channel impedances that have relatively low resistance, less than 40 Ω. Plus it is necessary to implement high-pass filter and PID controller to achieve the best result of the impedance matching.

CHAPTER 5

CONCLUSION

The use of adaptive impedance matching circuit in narrowband power line communication helps the system to achieve maximum power transfer in the power line network. By all means, it reduces the impedance mismatch in the system, thus less data reflection in the power line network. However, channel impedance in the low voltage network is time and location variant; hence it is rather difficult to match the impedance accordingly at all times. This thesis investigated the significance and problems of the current applications of adaptive impedance matching circuits, and following by the proposal of two new methodologies of adaptive impedance matching circuits. Furthermore, the formula given in the [8] for impedance measurement was simplified in this thesis.

In Chapter 3, the RLC band-pass filter adaptive impedance matching circuit was proposed. The impedances were matched using the digital capacitor and digital resistor. This method has relatively simple and clear mathematic algorithm to match the source and channel impedances continuously. By comparing with other existing adaptive impedance matching method, this method has advantage in higher matching resolution and easier to control. This method had been tested and verified using PSIM, MATLAB and laboratory experiments. However, the RLC circuit is only applicable if the impedances are consisting of pure resistive load only. In other words, if the reactance load in the channel impedances is negligible, then it is indeed a good method to be applied in the application of narrowband power line communication.

The improvement of the RLC band-pass filter impedance matching circuit was addressed in Chapter 4. The LCRC adaptive impedance matching circuit was introduced to match the source impedance with load impedance that consists of both resistive and reactance load. Since it introduces active inductor and additional digital capacitor, it has better matching resolution than the method shown in Chapter 3. It also presents versatile design of the filter by introducing parameters in resistance and capacitance. Besides, a new algorithm has been devised to adjust inductance only according to load and source impedance, which emphasizes flexibility design as well. The matching circuit also has the capability to filter out the noises and ensure the modulated frequency can pass through the circuit. However, it is more complex than the method given in Chapter 3. In addition to that, it requires high-pass filter and PID controller to ensure it performs in the ideal manner.

5.1 FUTURE WORK

The proposal of RLC band-pass filter adaptive impedance matching circuit from Chapter 3 uses the digital resistor and digital capacitor to match the source and load impedances in real time situation. Since it is only capable to match the resistive load, thus the LCRC adaptive impedance matching circuit from Chapter 4 was proposed to solve its limitation. But still LCRC adaptive impedance matching circuit has the limitation that only allow the impedance range within 40 Ω to perform in the ideal manner.

Hence, in potential future works for this research, it is necessary to investigate the characteristics of the PID controller that is suitable to be used in LCRC adaptive impedance matching circuit, with the purpose to improve not only the range of the impedances, but also the overshoot and the ringing effect in the step response of the circuit.

BIBLIOGRAPHY

[1] L. Chia-Hung, B. Ying-Wen, C. Hsien-Chung, and H. Chi-Huang, "Home appliance energy monitoring and controlling based on Power Line Communication," in *Consumer Electronics, 2009. ICCE '09. Digest of Technical Papers International Conference on*, 2009, pp. 1-2.

[2] S. Yuhao and G. A. J. Amaratunga, "High-current adaptive impedance matching in narrowband power-line communication systems," in *Power Line Communications and Its Applications (ISPLC), 2011 IEEE International Symposium on*, 2011, pp. 329-334.

[3] L. L. H.C. Ferreira, J. Newbury, T. G Swart,, *Power Line Communications: Theory and Applications for Narrowband and Broadband Communications Over Power Lines*: John Wiley & Sons, 2010.

[4] R. P. Joshi, S. Bhosale, and P. H. Patil, "Analysis and Simulation of Noise in Power Line Communication Systems," in *Emerging Trends in Engineering and Technology, 2008. ICETET '08. First International Conference on*, 2008, pp. 1287-1292.

[5] M. Katayama, T. Yamazato, and H. Okada, "A mathematical model of noise in narrowband power line communication systems," *Selected Areas in Communications, IEEE Journal on*, vol. 24, pp. 1267-1276, 2006.

[6] Y.-S. K. a. J.-C. Kim, "Characteristic Impedances in Low-Voltage Distribution Systems for Power Line Communication," *Journal of Electrical Engineering & Technology*, vol. 2, pp. 29-34, 2007.

[7] R. H. Scott R. Bullock, "Method and System for Power Line Impedance Detection and Automatic Impedance Matching," United State Patent 6515485, 2003.

[8] Q. Li, J. She, and Z. Feng, "Adaptive impedance matching in power line communication," in *Microwave and Millimeter Wave Technology, 2004. ICMMT 4th International Conference on, Proceedings*, 2004, pp. 887-890.

[9] C. Won-Ho and P. Chong-yeon, "A simple line coupler with adaptive impedance matching for Power line Communication," in *Power Line Communications and Its Applications, 2007. ISPLC '07. IEEE International Symposium on*, 2007, pp. 187-191.

[10] P. Chong-Yeun, J. Kwang-Hyun, and C. Won-Ho, "Coupling circuitary for impedance adaptation in power line communications using VCGIC," in *Power Line Communications and Its Applications, 2008. ISPLC 2008. IEEE International Symposium on*, 2008, pp. 293-298.

[11] L. Chia-Hung, C. Hsien-Chung, B. Ying-Wen, and L. Ming-Bo, "Power Monitoring and Control for Electric Home Appliances Based on Power Line Communication," in *Instrumentation and Measurement Technology Conference Proceedings, 2008. IMTC 2008. IEEE*, 2008, pp. 2179-2184.

[12] Khairanirani, "Power Line Communication Network," vol. 33 kB, S. J. A. I. B. K. Listrik, Ed., ed: Wikipedia, 2010.

[13] W. D. Phil Sutterlin, "Power Line Communication Applications Study," E. Corporation, Ed., ed, 2000.
[14] B. Baraboi. (2013). *Narrowband Powerline Communication --Applications and Challenges - Part I*. Available: http://www.edn.com/design/wireless-networking/4408140/Narrowband-Powerline-Communication-Applications-and-Challenges-Part-I
[15] D. Shaver, "Low Frequency, Narrowband PLC Standards for Smart Grid - The PLC Standards Gap!," ed: Texas Instrument, 2009.
[16] Z. Kaspar, "Power-Line Communication - Regulation Introduction, PL Modem Implementation and Possible Application ", F. r. a. t. C. E. 50065-1, Ed., ed, 2002.
[17] B. Baraboi. (2013). *Narrowband Powerline Communication - Applications and Challenges - Part II*. Available: http://www.edn.com/design/wireless-networking/4410990/Narrowband-Powerline-Communication-Applications-and-Challenges-Part-II
[18] R. M. Vines, H. J. Trissell, L. J. Gale, and J. Ben O'neal, "Noise on Residential Power Distribution Circuits," *Electromagnetic Compatibility, IEEE Transactions on*, vol. EMC-26, pp. 161-168, 1984.
[19] L. Selander and EnerSearch, *Power-line Communication: Channel Properties and Communication Strategies*: EnerSearch, 1999.
[20] M. P. Sibanda, P. A. Janse van Rensburg, and H. C. Ferreira, "Passive, transformerless coupling circuitry for narrow-band power-line communications," in *Power Line Communications and Its Applications, 2009. ISPLC 2009. IEEE International Symposium on*, 2009, pp. 125-130.
[21] M. P. Sibanda, P. A. Janse van Rensburg, and H. C. Ferreira, "Impedance matching with low-cost, passive components for narrowband PLC," pp. 335-340, 2011.
[22] I. Rosu. (2011). *Impedance Matching* [Notes]. Available: http://www.qsl.net/va3iul/Impedance_Matching/Impedance_Matching.pdf
[23] S. P. Thompson and T. Phillips, *Dynamo-Electric Machinery; a Manual for Students of Electrotechnics*: BiblioBazaar, 2009.
[24] N. N. B. P. R. Chin, A. K. M. Wong, K. I. Wong, "Adaptive Impedance Matching Network with Digital Capacitor in Narrowband Power Line Communication," presented at the IEEE International Symposium on Industrial Electronics (ISIE), Taiwan, 2013.
[25] D. M. Brown, W. E. Engeler, and J. J. Tiemann, "High frequency MOS digital capacitor," in *Electron Devices Meeting (IEDM), 1974 International*, 1974, pp. 523-526.
[26] T. Haiting, Y. Ruiming, L. Feng, H. Zhigang, W. Sitong, L. Shunxin, *et al.*, "Measurement on narrow band power line communication channel impedance of distribution network," in *Consumer Electronics, Communications and Networks (CECNet), 2011 International Conference on*, 2011, pp. 454-457.
[27] A. Antoniou, "Gyrators using operational amplifiers," *Electronics Letters*, vol. 3, p. 350, 1967.
[28] A. Antoniou, "Realisation of gyrators using operational amplifiers, and their use in RC-active-network synthesis," *Electrical Engineers, Proceedings of the Institution of*, vol. 116, pp. 1838-1850, 1969.

[29] "Analog Filter," in *Linear Circuit Design Handbook*, H. Zumbahlen, Ed., 1 ed: Analog Devices, Inc., 2007, p. 960.
[30] B. I. Saeed and B. Mehrdadi, "Zero overshoot and fast transient response using a fuzzy logic controller," in *Automation and Computing (ICAC), 2011 17th International Conference on*, 2011, pp. 116-120.

Every reasonable effort has been made to acknowledge the owners of the copyright material. I would be pleased to hear from any copyright owner who has been omitted or incorrectly acknowledged.